Development Advance Online Articles. First posted online on 6 July 2017 as 10.1242/dev.147942
Access the most recent version at http://dev.biologists.org/lookup/doi/10.1242/dev.147942

Cell interactions, signals and transcriptional hierarchy governing placode progenitor induction

Mark Hintze, Ravindra Singh Prajapati, Monica Tambalo[1], Nicolas A. D. Christophorou[3], Maryam Anwar[2], Timothy Grocott[4] and Andrea Streit*

Department of Craniofacial Development & Stem Cell Biology, King's College London, Dental Institute, London SE1 9RT UK

* corresponding author: andrea.streit@kcl.ac.uk

1: current address: The Francis Crick Institute, Mill Hill Laboratory, The Ridgeway, Mill Hill, London NW7 1AA UK

2: Imperial College London, MRC Clinical Sciences Centre, Hammersmith Hospital, London W12 0NN

3: current address: INRA, Institut Jean-Pierre Bourgin, UMR 1318, ERL CNRS 3559, Saclay Plant Sciences, RD10, Versailles, France

4: current address: University of East Anglia, School of Biological Sciences, Norwich NR4 7TJ UK

Keywords: chick embryo, cell fate, sense organs, sensory ganglia, transcriptional networks, signalling

Summary Statement

Combining embryological and network inference approaches we unravel the transcriptional and signalling hierarchy during placode progenitor induction and propose a new model for this process.

Abstract

In vertebrates, cranial placodes contribute to all sense organs and sensory ganglia and arsise from a common pool of Six1/Eya2+ progenitors. Here we dissect the events that specify ectodermal cells as placode progenitors using newly identified genes upstream of the Six/Eya complex. We show that two different tissues, the lateral head mesoderm and the prechordal mesendoderm, gradually induce placode progenitors: cells pass through successive transcriptional states, each identified by distinct factors and controlled by different signals. Both tissues initiate a common transcriptional state, but over time impart regional character and the acquisition of anterior identity depends on Shh signalling. Using a network inference approach we predict the regulatory relationships among newly identified transcription factors and verify predicted links using knock-down experiments. Based on this analysis we propose a new model for placode progenitor induction, in which the initial induction of a generic transcriptional state precedes regional divergence.

INTRODUCTION

During early development, many fate decisions are controlled by inductive interactions, whereby an inducing cell population instructs responding cells to change their fate. Neural induction is perhaps the best-studied inductive event, and several models have been proposed to explain the induction and patterning of the nervous system by the organizer (Stern, 2001). The "multiple organizer model" argues that different parts of the organizer induce distinct regions of the nervous system (Holtfreter, 1933a; Holtfreter, 1933b; Mangold, 1933; Saxen and Toivonen, 1962), while Waddington suggested a two-step model with "evocation" generating a generic, non-regionalised nervous system, followed by "individuation" to impart regional character (Waddington and Needham, 1936). Nieuwkoop's activation-transformation hypothesis suggests that initial induction generates anterior character, which is then posteriorized (Nieuwkoop and Nigtevecht, 1954). Currently, there is support for modified versions of both Nieuwkoop's and Mangold's models (Stern, 2001; Takemoto et al., 2006). However, the question remains whether these models could also explain the development of adjacent structures, the sensory placodes. Placodes arise in the head ectoderm in register with the neural tube and generate components of sense organs and cranial sensory ganglia (Baker and Bronner-Fraser, 2001; Grocott et al., 2011; Schlosser, 2010; Streit, 2008). Pushing the 'multiple organizer model' to the extreme, it has been suggested that even placodes are induced by a subset of organizer cells (Mangold, 1933; Saxen and Toivonen, 1962; Spemann, 1938). Here we ask whether placodes are induced by a bona fide organizer that induces and patterns the placodal territory, and if so, which if any of these models explains this process.

Although contributing to diverse organs and ganglia, the cranial placodes arise from a common domain, the pre-placodal region (PPR), which is specified at head process stages as a strip of ectoderm surrounding the anterior neural plate (Baker and Bronner-Fraser, 2001; Grocott et al., 2012; Schlosser, 2010; Streit, 2008). PPR cells initially have the same developmental potential: they can give rise to any placode and express a common set of genes (Bailey et al., 2006; Bailey and Streit, 2006; Streit, 2008), among them Six and Eya factors, which impart PPR character to ectodermal cells

(Brugmann et al., 2004; Chen et al., 2009; Christophorou et al., 2009; Laclef et al., 2003; Zheng et al., 2003; Zou et al., 2004; Zou et al., 2006). Surprisingly, few upstream regulators have been identified to explain how their expression is activated in and confined to sensory progenitors. *Six1* transcription is directly activated by Dlx-factors, but repressed by Msx1 (Sato et al., 2010). At gastrulation stages, BMP signalling is required for the PPR 'competence factors' *Gata2/3*, *Tfapa/c*, *Foxi1* and *Dlx3*, but must be inhibited later for *Six1* activation (Ahrens and Schlosser, 2005; Brugmann et al., 2004; Kwon et al., 2010; Litsiou et al., 2005; Pieper et al., 2012). Subsequently, FGF signalling together with BMP- and Wnt-inhibition is necessary for PPR formation and sufficient to induce sensory progenitors in non-placodal ectoderm (Brugmann et al., 2004; Litsiou et al., 2005). These signals emanate from the adjacent neural plate and the underlying head mesoderm (Ahrens and Schlosser, 2005; Litsiou et al., 2005), although their relative contribution to PPR induction remains unclear, as does the question of whether the signalling tissues are true organizers.

Using an established induction assay, we now dissect PPR induction and propose a new model. First, we design a molecular screen to identify new potential players and then use these factors to characterise the response to each PPR-inducing tissue and to establish a genetic hierarchy upstream of the Six/Eya complex. Combined with a network inference approach our analysis proposes a new multi-step model for PPR induction. We show that signals from the neural plate are unable to induce a PPR. Two different mesodermal populations, the lateral head mesoderm and the prechordal mesendoderm, initially induce a similar set of transcription factors (reminiscent of an "evocation"), but then gradually impart anterior and posterior bias to sensory progenitors ("individuation"). We show that PPR induction is not mediated by an 'organizer', but instead involves multiple signalling centres, each inducing cells with distinct regional character.

RESULTS

A molecular screen reveals the complexity of PPR induction

In chick, PPR induction is mediated by signals from the head mesoderm: when grafted next to competent epiblast this mesoderm induces a full set of bona-fide PPR markers (Litsiou et al., 2005). How long does this process take? In the same induction assay, quail lateral head mesoderm (lHM) requires at least 12 hrs of contact to induce the PPR markers *Six1* and *Eya2* in chick epiblast (Fig. 1A-C, b', c'; *Six1*:, 2/9; 8 hrs, 8/8; *Eya2*: 8 hrs: 0/7; 12 hrs: 3/10; *Six4*: 4hrs, 2/9; 8 hrs, 10/12 – not shown). To identify the components of the PPR induction cascade, we performed a microarray screen comparing the transcriptomes of epiblast from four conditions (Fig. 2C): mesoderm-induced epiblast (12 hrs; MIE), non-induced epiblast (control; NIE) from the contralateral side of the same embryos, and the normal anterior (aPPR) and posterior PPR (pPPR) at HH5/6 (Lleras-Forero et al., 2013). One-way-ANOVA reveals 3475 probes with a significant change of more than 2-fold ($p<0.05$) in at least one cell population representing 2868 unique transcripts including 206 known or putative transcription factors (Table S1; GSE81023). When compared to control epiblast, 1098 transcripts are mesoderm-induced (>1.2-fold), while 1379 genes are repressed (Table S2). As expected, the PPR enriched factors *Eya2, Dach1* and *Sox3* (Rex et al., 1977, Barembaum and Bronner-Fraser, 2007; Litsiou et al., 2005) are induced by the lHM, while neural crest (*Snail2*), neural plate (*Sox2*) and regionally restricted genes (*Pax6*) are not (Litsiou et al., 2005) (Fig. S1). Thus, the array screen replicates known changes in gene expression in response to mesodermal signals.

To ensure that the genes identified were induced by mesoderm rather than recruited from the host PPR, the screen was designed using extraembryonic tissue. However, for any gene to be relevant to PPR formation it should at some point be expressed in the prospective PPR. To identify synexpression groups we performed hierarchical clustering on all genes changing significantly and in situ hybridisation to verify their spatio-temporal expression in normal embryos. In total, we assessed

the in situ expression of 47 known or putative transcription factors, five chromatin modifiers and four signalling pathway components.

This analysis reveals seven major clusters with distinct profiles (C1-C7; Figs. S1, S2 and S3; Table S1, S5). C1 and C2 transcripts are largely absent from placode progenitors, like *Cux1* (C2; Fig. 2d), and repressed by the mesoderm, with C2 genes being enriched in the extraembryonic ectoderm (Fig. 2D). Cluster C5 transcripts (Fig. 2F) are strongly enriched in the aPPR, but only weakly mesoderm-induced, and include aPPR-specific genes like *Pax6* and *SSTR5* (Lleras-Forero et al., 2013), *Nfkb1* (Fig. 2f) and *Sall1* (Fig. S2). In contrast, cluster C6 transcripts (Fig. 2G) are lHM-induced, enriched in the pPPR and contain *Gbx2*, *Irx2* and *Pax7* (Goriely et al., 1999; Khudyakov and Bronner-Fraser, 2009; Steventon et al., 2012), and novel transcripts like *Znf423, Znf76* and *Rnf24*. Finally, cluster C4 genes are mostly induced by mesodermal signals and are present in the entire PPR. In situ hybridisation reveals that most C4 transcripts are not restricted to sensory progenitors, but expressed broadly at primitive streak stages encompassing the future neural, neural crest and placode territories (Fig. 2E, e; Figs. S2, S3) including *Zic1* (Khudyakov and Bronner-Fraser, 2009), *Otx2* (Bally-Cuif et al., 1995) and *Fzd8* (Paxton et al., 2010) and many new genes (Figs. S2, S3). Only a few C4 transcripts are restricted to the PPR (*Dmbx1*, *Homer2*; Fig. S3). As development proceeds some transcripts remain expressed in both neural and placode cells, while others become confined to either tissue (Figs. S2, S3), suggesting that Six and Eya factors are among the few bona-fide PPR markers.

Thus, the screen has identified many novel transcripts expressed in placode progenitors revealling molecular similarity between precursors for the central and peripheral nervous system. In addition, ultimately the lHM appears to induce posterior placode progenitors, but does not act as an organizer that induces and patterns the PPR. This finding implies that other PPR-inducing tissues exist, which should impart rostral PPR identity.

Prechordal mesendoderm induces placode progenitors

Endodermal signals have been implicated in anterior placode induction in amphibians (Henry and Grainger, 1990; Jacobson, 1963a; Jacobson, 1963b) and we have recently shown that the anterior prechordal mesendoderm (pME) is required for *Eya2*, *Pax6* and *pNoc* expression in chick and zebrafish (Lleras-Forero et al., 2013). To test its PPR-inducing ability, we grafted quail HH5 pME next to chick extraembryonic epiblast ($HH3^+/4^-$; Fig. 1D). Both *Six1* (5/8) and *Eya2* (7/8) are induced after 15-17hrs (Fig. 1D, d', E, e'). Thus, two different mesodermal tissues - lHM and pME - mediate PPR induction.

Lateral and axial mesoderm provide regional bias to sensory progenitors

Our results indicate that PPR induction is not mediated by an organizer, however it remains possible that lHM first induces aPPR, which is subsequently posteriorized. Alternatively both mesoderms may first induce generic PPR character, which is then regionalised, or each directly induces distinct rostro-caudal identity. To distinguish these possibilities and to capture the complexity of PPR induction, we compared the response to both tissues over time assessing 126 genes simultaneously. HH5/6 lHM or pME was grafted into the extraembryonic region of $HH4^-$ hosts and the underlying epiblast was collected after 3, 6 and 12 hrs, together with the contralateral control epiblast. Each experiment was performed in triplicate and gene expression was analysed by NanoString using a probe set containing known and new PPR transcripts, markers for different placodes, neural crest and neural plate (Table S3). Transcripts with a difference greater than 1.2-fold (p-value <0.05) between induced and time-matched control tissues were considered as differentially expressed.

The transcriptional hierarchy in response to the lateral head mesoderm

LHM derived signals initiate a dynamic response with distinct groups of transcripts being regulated at each time point (Fig. 3A-E; Table S4). At 3 hrs, only a few factors are upregulated: *Ccnd1*, *Etv5*,

ERNI, *N-myc*, *Otx2*, *Sall4*, *Trim24* and *Zic3* (Fig. 3B, c', c''). While some genes are maintained, others are only transiently induced: *Otx2* expression levels are negligible (Fig. S4) and *Sall4* disappears after 6 hrs, as do *ERNI* and *Zic3* after 12 hrs (Fig. 3B). At 6 hrs, new transcripts appear in response to the mesoderm (*Dnmt3b*, *Pdlim4*, *Irx2, Rybp, Stox2, Znf462*; Fig. 3B, d', d''; Table S4) while PPR genes (*Six1/4*, *Eya2*) are only upregulated after 12 hrs together with some of their known upstream regulators (*Gata3*, *Foxi3*, *tfap2a*, *Dlx6* (Kwon et al., 2010; Pieper et al., 2012; Qiao et al., 2012; Sato et al., 2010)]; Fig. 3B, e', e'') and genes previously not associated with PPR induction (*AATF, Bcl7a, Zhx2*; Fig. 3B, Table S4). In contrast, other genes are downregulated by the lHM (3hrs) including *tfap2a*, *Dlx5*, *Gata2* and *Axin2* (Fig. 3B; Table S4). At 12 hrs most remain absent and other PPR repressors (*Msx1*, *Bmp4*; (Ahrens and Schlosser, 2005; Litsiou et al., 2005; Sato et al., 2010) are reduced, however, *tfap2a* is now induced and *Dlx5* is no longer repressed consistent with their role as positive *Six1* regulators (Kwon et al., 2010; Qiao et al., 2012) (Fig. 3B; Table S4).

To determine the character of the lHM-induced cells we examined the normal expression patterns of all genes in each cohort, considering their dynamic changes and that at different times of development they may characterise different cell populations (summarised in Figs. S2, S2 and Table S5). This analysis reveals that 3 and 6hr-induced transcripts are normally expressed early and broadly: at HH3-4 their domains encompass the presumptive neural plate and its border including future neural crest and placodes (Fig. 3C, c''', D, d'''; Figs. S2, S3; Table S5), except *ERNI* and *Otx2*, which are already expressed in the pre-streak epiblast and then label much of the epiblast and the anterior ectoderm, respectively (Bally-Cuif et al., 1995) . Most factors are maintained in the neural plate and/or PPR at head fold stages (HH6/7; Figs. S2, S3; Table S5). In contrast, most 12hr-induced transcripts first appear at HH5/6 (*Six1*, *Six4, Eya2*) or begin broadly in the non-neural ectoderm (*Gata3*, *Dlx6*, *Homer2*, *Foxi3*) to become confined to or upregulated in the PPR (Fig. 3E, e'''; Table S5). Most mesoderm-induced genes are present in all placode progenitors, however *Foxi3* (Khatri et al., 2014) and *Gbx2* (Steventon et al., 2012) are restricted to future otic and epibranchial cells by the time PPR markers are expressed; *Otx2* remains present, however at extremely low levels (Fig. S4).

Thus, at PPR stages the normal expression of all 12 hr induced genes overlaps in the posterior PPR suggesting that the induced tissue has acquired posterior PPR character.

Together these data reveal that the lHM gradually induces PPR identity with cells passing through sequential states. The first step does not generate anterior character, but resembles preprimitive streak or early streak stage epiblast and a posterior PPR is established over time.

The transcriptional hierarchy in response to the prechordal mesendoderm

We observe a similar hierarchy in response to the pME. 3 hours after grafting, the mesendoderm induces the same transcripts as the lHM (Fig. 4A, B, c', c''; Table S4), with most genes being maintained until at least 12 hrs. The mesendoderm appears to induce *Irx1*, *Gbx2* and *Sstr5* albeit at extremely low levels (Fig. 4B; Figs. S4 and S5; Table S4). This is followed by induction of 17 transcripts including PPR genes (*Six1*, *Eya2*, *Irx1*, *Homer2*; Fig. 4B, d', d'') and finally by many genes at 12 hrs including the Six1 co-factor *Dach1* (Fig. 4B, e', e''; Table S4). The pME represses the same genes as the lHM although the timing varies slightly (compare Figs. 3B and 4B).

In normal embryos, 3hr pME-induced genes are expressed widely at HH3/4 labelling the future neural plate and its border (Fig. 4C, D, c'''; Figs. S2 and S3; Table S5). 6hr-induced genes overlap in the PPR (Fig. 4D, d'''), although two neural transcripts (*Sox2*, *Znf423*) are also present (Table S5). Most 12hr-induced genes continue to overlap in the PPR and the presence of *Otx2*, *pNoc*, *SSTR5* and *Six3* suggests that cells have acquired anterior character (Fig. 4E, e'''). However, in addition, seven induced genes are normally confined to the neural plate (Table S5). Thus, the pME rapidly induces aPPR, but overtime generates tissue of mixed (neural/pre-placodal) anterior identity. The delayed induction of neural character excludes the possibility that an induced neural plate contributes to the accelerated induction of PPR transcripts by axial mesendoderm versus lHM. In summary, like the lHM, the pME initiates a sequence of transcriptional responses until PPR identity is established. Both tissues initially induce a small set of common transcription factor (Fig. S5), but subsequently impart anterior and posterior bias.

Neural plate signals are not sufficient induce placode progenitors

The neural plate has been implicated in PPR induction in *Xenopus* (Ahrens and Schlosser, 2005), however this does not appear to be the case in chick (Litsiou et al., 2005). We now revisit this question using our newly identified genes. The future forebrain (aNP) or hindbrain (pNP) from HH5/6 donors was grafted into the extraembryonic region of $HH4^-$ hosts; epiblast exposed to neural plate signals was dissected together with non-induced epiblast from the contralateral side after 3, 6 and 12 hrs and processed for NanoString analysis (Fig. S6; Table S4).

After 3 hrs, the aNP induces many newly identified transcripts, as well as FGF mediators (*Etv4*, *Etv5*) and the crest marker *Pax7* (Fig. S6). Except for *Stox2* and *Mynn*, which are absent from the central-most epiblast, all other factors are normally expressed broadly at HH3/4 in the future neural plate and its border (Figs. S2, S3; Table S5). Most genes differ from mesoderm-induced transcripts and are only transiently activated. Likewise, five 6hr-induced transcripts are broadly expressed in the HH4 epiblast, while three (*Hey1*, *Foxi3*, *Six1*) are confined to the PPR. This is followed by many genes whose normal expression does not overlap in a single territory including NP-specific transcripts (HH5/6; *Sox2*, *Znf423*) and non-neural ectoderm genes (*Gata3*, *Pax6, Irx1*, *Eya2*). The PPR marker *Six1* is no longer induced, while other PPR-specific genes never respond to aNP grafts (*Six4*, *Homer2*). Finally, the aNP represses known *Six1* regulators (*Dlx5*, *tfap2a*; (Kwon et al., 2010; Qiao et al., 2012; Sato et al., 2010). Therefore, aNP-derived signals induce a mixture of neural and neural plate border cells rather than a unique territory and cannot initiate a complete PPR.

Similar results are observed in response to pNP-derived signals (Fig. S6). After 3 hrs, 28 genes are initiated, which are expressed widely in the normal embryo at HH3/4 (Table S5), except the neural plate border gene *Irx1*. Many transcripts continue to be present 6 and 12 hrs after pNP grafts, while 11 transcripts are only transiently induced. This is followed by neural plate (*Sox2*, *Zic2*, *Znf423*) and/or border genes ($HH4^+$/5) with *Eya2* being the only pNP-induced PPR marker.

Simultaneously non-neural markers and *Six1* regulators (*Gata2*, *Dlx3/5*, *Tfap2a*) are repressed. Thus, the pNP induces a territory of mixed identity including many neural and non-neural transcripts with *Gbx2 and Irx2* indicating a posterior bias. Thus, like the aNP, the pNP induces different cell populations or cells with mixed identity (neural/placodal). Initially aNP and pNP grafts induce distinct transcripts, while there is significant overlap later (Fig. S6). In summary, the neural plate induces many genes, however unlike the mesoderm it cannot induce the full transcriptional profile characteristic of placode progenitors.

Integration of signalling pathways during PPR induction

FGFs together with BMP and Wnt antagonists have previously been implicated in PPR induction (Brugmann et al., 2004; Kwon et al., 2010; Litsiou et al., 2005). Having identified distinct transcriptional states as cells adopt sensory precursor identity, we can now dissect the role of each signal at different time points by combining mesoderm grafts with pathway manipulation.

FGF initiates PPR induction

FGF signalling is required for PPR induction (Litsiou et al., 2005). To test which genes are FGF-induced, we grafted FGF8-coated beads into HH4^{-} extraembryonic region and analysed FGF8-exposed and control epiblast gene expression after 3 and 6 hrs using NanoString. After 3 hrs, FGF8 induces a few genes (D: black arrows; Fig. S7; *Etv5, Trim24, Ccnd1, ERNI, N-myc, Sall4*), largely overlaping with lHM- (6/8) and pME-induced (5/7) transcripts. *ERNI* is already known to be modulated by FGF8 (Streit et al., 2000). At 6 hrs *Etv5, Ccnd1, N-Myc* and *Trim24* continue to be upregulated, as are some additional transcripts (*Stox2, Cited2, Znf462*) (Fig. 5D, Fig. S7). We confirmed the induction of *Trim24* (Fig. 5A-A''; 4/4) and *N-myc* (not shown; 6/9) by in situ hybridisation. In contrast, FGF8 – like the mesoderm - represses *tfap2a*, *Dlx3*, *Dlx5*, *Gata2* and *Axin2* (Fig. 5D, Fig. S7; Table S4).

To assess the requirement of FGF signalling we combined lateral or axial mesoderm grafts with control beads or beads coated with the FGF-receptor antagonist SU5402 (Fig. S7; Table S4). Both tissues induce *Etv5* and *N-myc*, however the requirement (blue arrows) for FGF signalling differs: while FGF signalling is necessary for *Etv5* induction by the lHM (Fig. 5B-B''), it is not required for its induction by the pME, while the opposite is true for *N-myc* (Fig. 5D-E; Fig. S7; Table S4). *ERNI* induction by the lHM requires FGF signalling as do pME-induced genes (*Sox3*, *Homer2*) and the neural genes *Sox2*, *Zic2* and *Zic3* (Fig. 5D, E; Fig. S7; Table S4). Finally, FGF signalling is necessary *Gata2* repression by both tissues, for *tfap2a* suppression by the lHM and for inhibition of *Msx1* and *Axin2* by the pME (Fig. 5D, E; Fig. S7; Table S4). Together, these results show that FGF signalling is sufficient to induce or repress many genes that characterise the earliest response to mesoderm-derived signals (Fig. 5D, E; Fig. S7). However, only a few transcripts strictly depend on FGF suggesting that each tissue contains other signals that can compensate for FGF loss.

BMP antagonism is required throughout PPR induction

The role of BMP signalling in PPR formation changes over time: during gastrulation it is required to induce Six/Eya regulators, but subsequently must be reduced to allow the emergence of sensory progenitors (Ahrens and Schlosser, 2005; Brugmann et al., 2004; Kwon et al., 2010; Litsiou et al., 2005). To test which mesoderm response genes change after BMP pathway modulation, we reduced BMP signalling by growing primitive streak stage embryos in the BMP inhibitor Dorsomorphin. After 3 and 6 hrs' culture, 11 transcripts are upregulated in PPR-competent epiblast when compared to stage-matched controls (Table S4). However, of these only *Trim24* is induced by both mesodermal tissues (see Fig. 3c').

To test which mesoderm-induced genes require BMP antagonism, we compared the inducing ability of mesoderm alone or mesoderm together with BMP4 coated beads after 3 and 6 hrs. BMP activation leads to the loss of *Trim24, CCDN1, Sall4, Otx2, ERNI* and *Zic3* induction by the lHM (Fig. 5D; Fig. S7; Table S4); we confirm the reduction of *Trim24* by in situ hybridisation (Fig. 5C-

C''). Of pME-induced 23 transcripts, ten are repressed after BMP activation including *Trim24*, *N-myc* and the PPR genes *Six1* and *Eya2* (Fig. 5E; Fig. S7; Table S4). Likewise, the downregulation of some transcripts by the lHM is sensitive to BMP activation: *Dlx3*, *Dlx5* and *Gata2* increases when compared to control grafts (Fig. 5D; Fig. S7). In contrast, the pME continues to suppress Dlx genes even at elevated BMP levels, while *Msx1* and *Axin2* inhibition requires BMP antagonism (Fig. S7). Therefore, although BMP inhibition alone is sufficient to activate only few mesoderm-induced genes, many transcripts require BMP antagonism among them both early and late mesoderm response genes. In addition, these findings highlight that although both mesoderm populations induce similar sets of transcription factors, each tissue provides a distinct signalling environment where other signals can compensate for the loss of particular pathway.

Wnt antagonism is not required during early PPR induction

At the border of the neural plate increased levels of Wnt signalling promote neural crest formation at the expense of PPR, while Wnt antagonists have the opposite effect (Litsiou et al., 2005). To test which transcripts respond to Wnt modulation at different time points, we exposed the extraembryonic epiblast to the Wnt antagonist IWR and compared gene expression to control, untreated epiblast using NanoString after 3 and 6 hrs. Wnt inhibition results in the upregulation of several genes including *Dlx5* and *Nfkb1* as well as the Six1 co-factor *Dach1* (Table S3). However, none of these are induced by mesoderm grafts suggesting that antagonising Wnt signalling does not mimic the response to mesoderm signals.

To assess whether mesoderm-induced genes depend on Wnt antagonism, we combined tissue grafts with control DMSO-coated beads or beads coated with the Gsk3 inhibitor BIO to activate canonical Wnt signalling. Only a few genes, normally induced after 6 hrs, are affected: *Rybp* is no longer induced by the lHM, while *Sox3* is no longer upregulated by the pME (Fig. 5D-E; Table S4; Fig. S7). Thus, modulation of Wnt signalling does not play a major role during the initial phase of

PPR induction, but may be important for the decision between neural crest and placode progenitors (Litsiou et al., 2005; Villanueva et al., 2002).

Sonic hedgehog signalling is required for anterior PPR induction

The above experiments demonstrate that the axial mesendoderm is important to imbue sensory progenitor cells with anterior character. What is the nature of the anteriorising signal? Mesendoderm-derived somatostatin mediates PPR induction, but does not impart regional identity (Lleras-Forero et al., 2013). Since sonic hedgehog (shh) is prominently expressed in the pME (Dale et al., 1997), we tested whether it is required for aPPR formation. We grafted pME next to competent epiblast of HH4- hosts with or without cyclopamine, an shh inhibitor (Fig. 6 A-C). After 16 hrs, the general PPR markers *Six1* (Fig. 6 A; *Six1*: 7/9) and *Eya2* (not shown) continue to be induced, while the anterior markers *Six3* and *Otx2* are reduced (Fig. 6 B-C; Six3: 8/11; Otx2: 4/4). Shh-coated beads are not sufficient to induce PPR or anterior markers in the extraembryonic epiblast. We therefore tested whether Shh can anteriorise the lHM-induced PPR. When lHM grafts are combined with Shh-coated beads the anterior marker Six3 is not induced (Fig. S11). Together, these data indicate that Shh alone is not sufficient to impart anterior identity or induce sensory progenitors, but plays a role in conferring rostral character to the PPR.

Network predictions support a transcriptional hierarchy during PPR induction

Our analysis suggests a gradual transition of epiblast cells towards placode progenitor fate, each step defined by distinct transcriptional regulators and controlled by a combination of signals. Based on time course analysis we propose that at the top of the hierarchy a small set of transcription factors defines an 'primed ectoderm state' and controls the expression of a second tier of factors, which then directly regulate the Six/Eya cassette in the PPR. To test this model, we used an unbiased approach to investigate the topology of the PPR genetic network.

Using the NanoString datasets we inferred a regulatory network using the GENIE3 algorithm (Huynh-Thu et al., 2010). We created a network using all interactions with an importance measure of 0.02 or higher (Fig. S8A), which highlights important nodes (potential regulators) and weighted directional interactions. Visual inspection suggests the existence of three potential sub-clusters, which indeed emerge upon further dissection of the network using community clustering (Fig. S8, cluster G1-G3). *Six1*, *Six4*, *Eya2* and other PPR-specific genes cluster together with known Six1 upstream regulators (Fig. S8C, cluster G2). In addition, G2 contains several early mesoderm response genes including *Otx2*, *ERNI*, *Sall1*, *Sall4*, *CCND1*, *Trim24*, *Zic3* and the FGF mediators *Etv4* and *-5* (Fig. S8C). Thus, the network predictions correlate well with our proposed model.

To assess potential direct regulators of *Six1* and *Eya2*, we extracted their nearest neighbours from the network (Figs. S8A, S9). Using this information together with our induction time course and the spatial information from in situ hybridisation, we constructed a gene regulatory network in BioTapestry (Fig. 7 A). Genes not induced by the mesoderm or not co-expressed with *Six1* and *Eya2* (e.g. *Hey2, Irx1*) were excluded from the BioTapestry network as potential direct interactors. Many first neighbours are shared by *Six1* and *Eya2* including known upstream regulators like *Gata3* and *Dlx6* (Kwon et al., 2010; Sato et al., 2010). In addition, the network predicts novel regulatory relationships between the *Six1-Eya2* complex and *Sall1, Gbx2*, *Hey1* and *Hesx1*. To corroborate these predictions, we analysed the transcription factor binding sites of the only PPR enhancer so far identified, *Six1-14* (Sato et al., 2010), which directs its expression in the anterior PPR. This analysis confirms the presence of Gata, Dlx, Gbx and Sall motifs (Table S6) indicating that these factors may indeed directly regulate *Six1* (Fig. 7A, bottom: 12 hrs, purple/pink genes).

In contrast, none of the early mesoderm response genes defining the primed ectoderm state (*Etv5, Otx2, Zic3, N-myc, Trim24*; Fig. 7A top: 3hrs, blue genes) are predicted to interact with *Six1* and *Eya2* directly. We therefore analysed their first neighbours in the GENIE3 network as well as those of the predicted direct *Six1*/*Eya2* regulators (*Gata3, Dlx6, Gbx2, Foxi3, Sall1*; Fig. S9). This analysis reveals a small set of intermediate transcripts downstream of the genes defining the primed

ectoderm, among them *Hesx1*, *Znf462*, *Hsf2*, *Pdlim4*, *Irx2*, *Cited2* and *Sox3*, which are all induced 6 hrs after exposure to mesodermal signals (Fig. 7D; middle: 6 hrs, purple/pink genes). In turn, they are connected to the *Six1*/*Eya2* regulators suggesting that they provide the link between 3- and 12 hr-induced genes. We have termed the transcriptional state where 3- and 6hr induced genes are co-expressed 'PPR-primed' state. In summary, our network inference approach supports a gradual transition of epiblast cells towards PPR fate and highlights the hierarchical nature of this process.

Confirming predicted interactions

To test whether these intermediate genes are regulators in the PPR gene network, we assessed the potential role of two transcription factors Znf462 and Pdlim4. We designed two different morpholinos for each factor to knock down their expression. Experimental or control morpholinos were electroporated at primitive streak stages, the anterior and posterior PPR was dissected at HH6/7 and analysed by NanoString. While reduction of Znf462 changes the expression of many transcripts when compared to controls (anterior PPR: 30; posterior PPR: 94), knock-down of Pdlim4 only affects nine genes (Table S4). This analysis verifies five of six predicted links downstream of Znf462 and one of two downstream of Pdlim4. To corroborate these findings we performed in situ hybridisation for selected genes after Znf462 and Pdlim4 knock-down. While control morpholinos have no effect (Fig. S10), the reduction of either gene prevents *Six1* and *Eya2* expression (Fig. 7C, E, F). Furthermore, Znf462 regulates *Foxi3* and *Pdlim4* (Fig. 7D, F): while Znf462 is required for *Foxi3*, it seems to repress *Pdlim4*. Finally, Pdlim4 knockdown leads to a reduction of *Dlx6* expression as predicted (Fig. 7B). Thus, these findings provide experimental support for the GENIE3-predicted gene regulatory network, and suggest that genes induced within 6hrs after mesoderm grafts link early response genes and PPR competence factors.

DISCUSSION

Sensory placode progenitors are specified at head process stages in the ectoderm surrounding the anterior neural plate (Baker and Bronner-Fraser, 2001; Grocott et al., 2012; Schlosser, 2010; Streit, 2008). Initially, they are competent to give rise to all cranial placodes and share common features, but as individual placodes emerge, their developmental potential becomes gradually restricted (Bailey et al., 2006; Bailey and Streit, 2006; Schlosser, 2010; Streit, 2008). Thus, induction of sensory progenitors is thought to be a common step that generates a non-regionalised placode territory, which is later subdivided along the rostro-caudal axis. Here, we provide evidence that PPR induction and regionalisation occur simultaneously suggesting that a homogeneous PPR without anterior-posterior identity does not exist. Having identified new genes in the regulatory cascade that specifies sensory progenitors, we investigate their temporal hierarchy. This allows us to dissect the events upstream of the PPR specifiers *Six1* and *Eya2* and reveals how signals from different tissues gradually induce placode precursors with distinct rostro-caudal identity.

A transcriptional hierarchy gradually specifies sensory placode progenitors with distinct rostro-caudal character

Three independent approaches – a PPR induction assay, gene expression during normal development and network analysis – lead us to propose a new multi-step model for PPR induction. Although we describe discrete steps as cells acquire PPR identity, it is likely that in reality the transitions between them are fluid and represent a continuum. In the first step, signals from the lHM and the pME rapidly induce a small set of transcription factors including *ERNI, Etv5, N-Myc, Otx2, Zic3* and *Trim24* (akin to 'evocation' in Waddington's model). These are largely identical irrespective of the signalling source suggesting that both tissues initially promote a common transcriptional state. In the normal embryo, these factors are expressed very early with their domains encompassing the future neural plate, neural crest and placode territory indicating that before

acquiring PPR identity cells pass through a 'primed ectoderm state' that is common to progenitors for both the central and peripheral nervous system. How this state is induced in the normal embryo remains to be elucidated, however our results raise the possibility that FGF signalling may, at least in part, mediate this process. FGF8 largely mimics the response to mesodermal signals (see Fig. 5), is required for the early, but not the late steps of PPR induction (Litsiou et al., 2005), and is known to initiate neural and neural crest formation (Delaune et al., 2005; Linker and Stern, 2004; Monsoro-Burq et al., 2003; Streit et al., 2000; Stuhlmiller and García-Castro, 2012; Wilson et al., 2000). It is thus possible that like neural induction, PPR formation starts much earlier than previously thought and our induction assay rapidly recapitulates normal development.

The second phase of PPR induction is characterised by a set of new transcription factors (Fig. 7D, middle), whose expression in the embryo starts after the genes defining the primed ectoderm, but is equally broad. Together, they characterise a transcriptional state we termed the 'PPR-primed state'. Among these the zinc finger transcription factor Znf462, which is induced by both the lateral head mesoderm and axial mesendoderm, emerges as a potential integrator in the PPR gene network: several early response factors are predicted to provide input to *Znf462*, while Znf462 itself regulates *Foix3* and is predicted to control *Gbx2, Gata3* and *Dlx6*, which in turn control *Six1* and *Eya2*. In this phase, PPR regionalization begins (akin to 'individuation' in Waddington's model) and under the influence of lHM and axial mesendoderm anterior-posterior markers are upregulated. Finally, bona fide PPR markers, *Six1/4*, *Dach1* and *Eya2*, are induced as are PPR competence factors (Bhat et al., 2013; Kwon et al., 2010; Litsiou et al., 2005; Pieper et al., 2012), which may regulate *Six1* directly. Thus, as different populations of mesoderm emerge from the primitive streak, they transform primed ectoderm into PPR with regional character, without inducing definitive placode fates.

While this hierarchical model emerges from an ectopic induction assay, epiblast cells go through the same transcriptional states as they gradually acquire PPR fate. Genes defining the primed ectoderm are present early, some before gastrulation (Grocott et al., 2012), followed by our

newly identified primed-PPR factors. Where the latter overlap with PPR competence factors (*Gata*, *Dlx*, *Tfap2a;* Bhat et al., 2013; Kwon et al., 2010; Pieper et al., 2012), PPR specifiers are induced. Competence factors are initially expressed in the entire non-neural ectoderm at low levels (Bhat et al., 2013; Kwon et al., 2010; Pieper et al., 2012), but their expression increases in sensory progenitors as development proceeds. Our network analysis suggest that this enhanced expression maybe controlled by the newly identified transcription factors like Znf462. Whether any of the competence or newly identified factors act as pioneer factors for the Six-Eya network remains to be elucidated.

This model for PPR induction somewhat resembles Waddington's model for neural induction, which proposes that the organiser initially induces a tissue of generic neural character and then imparts regional identity (Waddington and Needham, 1936). Although placode progenitor induction does not involve a bona fide organizer, but is instead mediated by different tissues, both initially induce a common transcriptional state (evocation) without rostro-caudal character, and subsequently impart regional bias (individuation). At this point PPR cells are specified as placode progenitors, but not yet committed to a specific placodal fate (for review: Bailey and Streit, 2006; Grocott et al., 2012; Streit, 2008). Together, our data propose that during PPR induction cells initially pass through a primed ectoderm state, characterised by only a handful of genes, followed by a PPR-primed state defined by newly identified transcripts like Znf462. Subsequently, mesoderm signals divert cells towards placode fate and simultaneously impart regional bias depending on their location along the rostro-caudal axis.

Tissues and signals in PPR initiation and regionalisation

Signals from the neural plate and the lateral head mesoderm have previously been implicated in placode progenitor induction (Ahrens and Schlosser, 2005; Litsiou et al., 2005). Here, we identify the prechordal mesendoderm as an inducer of anterior PPR fate. Assessing the behaviour of 126 transcripts simultaneously allows us to dissect the dynamic response to all three tissues and reveals

that, while mesodermal signals initiate the full set of PPR transcripts in the induction assay, the neural plate alone is not sufficient to do so. It is likely that in normal development signals from the neural plate contribute to PPR induction. However, our findings suggest that they may play a less prominent role in initiating induction, but may be important to define regional character of the tissue induced.

FGF signalling mimics some of the earliest responses to signals from the mesoderm, although it is strictly required for only few rapidly induced genes (Litsiou et al., 2005). While BMP inhibition is sufficient to induce only two transcripts, *Trim24* and *Irx1*, it is required for the induction of many more. Together, both pathways account for the majority of lHM-induced genes, and for a considerable number of transcripts initiated by the pME. In particular, our findings confirm that antagonising BMP signalling is critical for the expression of the PPR specifiers *Six1* and *Eya* (Ahrens and Schlosser, 2005; Brugmann et al., 2004; Litsiou et al., 2005). Together these results suggest that the cooperation of FGF activation and BMP antagonism is crucial during the early phase of PPR induction and that both contribute to establishing a primed-PPR state, but are not sufficient for PPR specification.

In contrast, Wnt signalling only appears to play a minor role during the first step of PPR specification. Wnt antagonism does not mimic any activity of the mesoderm and only very few genes depend on Wnt inhibition. This suggests that modulation of canonical Wnt signalling is important during the late phase of PPR induction, where it may mediate different processes. On one hand, Wnt antagonists mediate the decision between neural crest and placode precursors at the border of the neural plate and protect PPR cells from Wnts emanating from surrounding tissues (Brugmann et al., 2004; Litsiou et al., 2005). On the other hand, Wnt antagonism may also be important to promote posterior PPR identity. Although active Wnt signalling is generally considered to posteriorize neural and non-neural ectoderm (Wilson and Houart, 2004), Wnt inhibition may be required to fine-tune pre-placodal fate. Finally, while studies in zebrafish have implicated Shh in the decision between adenohypophysis and lens character (Dutta et al., 2005), our results suggest an even earlier role at

pre-placodal stages. Shh and somatostatin (Lleras-Forero et al., 2013) from the axial mesendoderm may cooperate to initiate *Nociceptin* in anterior PPR cells, which in turn is required for the expression of aPPR transcription factors.

Conclusion

In conclusion, the combination of embryological time course experiments analysing more than 100 genes and network analysis reveals a new multi-step model for PPR induction. We demonstrate that the acquisition of placode progenitor fate occurs gradually and that cells transit through different transcriptional states, each defined by distinct factors. The first step generates primed ectoderm cells, followed by a PPR-primed state, which may be shared with neural and neural crest induction. Subsequently, two different tissues, the pME and the lHM, gradually impart anterior and posterior PPR character, respectively. Thus, PPR induction and regionalisation occurs simultaneously suggesting that once induced PPR cells do not share the same transcriptional profile. However, since both tissues initially elicit an almost identical response and cells only diverge later, PPR induction is somewhat reminiscent of Waddington's evocation-individuation model for neural induction.

EXPERIMENTAL PROCEDURES

Embryo techniques and in situ hybridisation

Fertile hens' (Winter Farm) and quails' (Potter Farm) eggs were incubated at 38°C to obtain embryos of appropriate Hamburger and Hamilton (HH) stages (Hamburger and Hamilton, 1951). Chick embryos at stage $3^{+}/4^{-}$ were cultured according to New (New, 1955) as modified by Stern and Ireland (Stern and Ireland, 1981). To isolate quail and chick tissues for grafting embryos were collected in Tyrode's saline. LHM and pME was dissected from HH5/6 donors, using fine steel needles and small amounts of dispase (1mg/ml). Neural plate from different rostro-caudal levels was obtained from HH6 donors after removal of the endoderm and mesoderm. For fluorescently labelled grafts, tissue was collected as above and incubated for 45 minutes at 38°C in DMEM containing

10µM CMFDA. Tissues were kept on ice in Tyrode's saline until grafted into the inner margin of the extraembryonic area opaca of HH4$^-$ hosts.

To inhibit Wnt or BMP signalling whole embryos (HH4$^-$) were cultured in modified New culture with albumen containing 30µM IWR-1 or 20µM Dorsomorphin, respectively. Heparin beads were coated in 50µg/ml of FGF8 in PBS containing 0.1% BSA on ice for one hour, washed briefly in Tyrode's saline and grafted into the inner third of the area opaca of HH4$^-$ stage chick embryos. Heparin beads were coated with 100µg/ml Shh in PBS containing 0.1% BSA for one hour on ice, washed in Tyrode's saline and grafted into the area opaca alone or in combination with lHM. To modulate different signalling pathways AG1X2 beads were coated with 1µg/ml BMP4 in PBS containing 0.1% BSA for 1hr on ice, with DMSO (control), 25µM SU5402 in DMSO or 2.5µM BIO in DMSO at room temperature for 2hrs. Affi gel blue beads were coated with 1µM cyclopamine in DMSO for 2 hrs. Beads were then washed in phosphate buffered saline and grafted together with lHM or pME. SU5402 is yellow, and beads retain their colour upto at leat 6 hrs after grafting, but have released all inhibitor after 15 hrs and appear white. To ensure that BMP4 beads are effective over the 6 hr time course, we grafted beads next to the neural tube and assessed *Sox2* expression, (Fig. S11). The effectiveness of IWR and dorsomorhin was assessed after growing embryos from HH5/6 in the presence of these drugs and assessing heart and somite formation (Fig. S11). As positive controls for Shh and cyclopamine we grafted beads next to the node at HH4 and assayed for *Pitx2* expression after 12 hours' culture (Fig. S11).

For whole mount in situ hybridization embryos were harvested in phosphate buffered saline, fixed in 4% paraformaldehyde and processed for hybridisation using DiG-labelled antisense mRNA as previously described (Streit and Stern, 2001). EST clones were obtained transcribed as appropriate (Table S7). To reveal quail tissue QCPN antibody (1:5 dilution) was used (Developmental Studies Hybridoma Bank, maintained by the Department of Pharmacology and Molecular Sciences, The Johns Hopkins University School of Medicine, Baltimore, MD 21205 and the Department of Biological

Sciences, University of Iowa, Iowa City 52242, under contract N01-HD-2-3144 from NICHD; AB 531886).

Electroporation and morpholino knock-down experiments

Two independent fluorescein-labelled morpolinos were designed by GeneTools targeting Pdlim4 (MO1: 3'CGACACCACGTGCACCATACC5';MO2: 3'CATCCACTTAAAGCGGCTCCGAGGC5') andZnf462(MO1:3'AGACACACAGATCCTTACCCTCTCT5';MO2:3'TGCAGCACCTCCATGGTTCAAGGAT5'). These are splice-blocking morpholinos; blastN does not reveal any other potential targets and their effectiveness was assessed by RT-PCR. Control morpholinos used are 3'CCTCTTACCTCAGTTACAATTTATA5'. For electroporation, each morpholino (1μg/μl) was mixed with plasmid DNA (0.5mg/ml) as a carrier and 0.01% fast green, and injected between the vitelline membrane and the epiblast. Primitive streak stage embryos ($HH3^{+}/4^{-}$) were prepared for New culture; morpholinos were transferred into epiblast cells using with four 5mV pulses for 50ms, with an interval of 500ms. Tarteget cells are visualized by fluorescence or by immuno-staining with anti fluorescein antibodies. For NanoString analysis, electroporated anterior and posterior PPR was dissected from HH6/7 after electroporation.

Microarray analysis

To identify differentially regulated transcripts lHM was grafted into the area opaca of $HH4^{-}$ chick hosts. After 12 hours, mesoderm grafts were removed using small amounts of dispase and the underlying area opaca epiblast was collected together with control epiblast from the contralateral side. Tissue collection was repeated on three independent occasions, with 35-40 explants collected for each sample. Using 5ng of total RNA, labelled cell extracts were prepared and hybridized to Affymetrix Chick GeneChip (Chambers and Lumsden, 2009). Probe level values were derived from the raw data using the MAS5 algorithm (version 1.2; Affymetrix). Data were analysed using the GeneSpring package (version 7.3.1; Agilent Technologies, UK). The suitability of the data sets for

further analysis and the relationship between and within the biological replicates was determined using principle components analysis and hierarchical clustering. Differential expression between the conditions under investigation was determined by a step-wise process. Samples were first normalized to the 50th percentile across the whole expression dataset and then each gene was normalized to the median of its own expression across each cell type. Prior to statistical analysis, genes classed as being not expressed (absent in biological replicates) or not varying their expression above a twofold level in any of the cell types were removed from the analysis. From the remaining set genes, whose expression levels differ significantly between each cell type, were determined by one-way analysis of variance (ANOVA; $p = <0.05$). Data were deposited in Gene Expression Omnibus (GSE48116, GSE81023). Transcripts expressed in the anterior and posterior pre-placodal region have previously been identified (Lleras-Forero et al., 2013) (accession number GSE48116). For hierarchical clustering and heatmap generation the R-statistical packages Hclust and Heatmap.2 were used.

NanoString n-Counter

Area opaca exposed to signals from different tissues and non-induced area opaca explants were collected at 3, 6 and 12 hours after grafting. Three independent replicates of 5-10 explants (5000-10,000 cells) per condition were collected on ice in RNAse-free phosphate buffered saline, which was then replaced by lysis buffer (Ambion) and the lysed tissues were quickly spun before being snap frozen on dry ice. Samples were stored at -80°C until required. RNA lysates were hybridised at 65°C overnight, eluted according to the nCounter manual and counted by the nCounter digital analyser. Counts were normalised to the positive and controls present in each hybridisation mix. Subsequently, the negative control probe values were used to create a background threshold level; transcripts with expression values below the threshold were removed from further analysis. Counts were then normalised to the total amount of mRNA counted in each sample. Differential expression

of transcripts between different conditions was determined using an unpaired students t-test -two-tailed -comparing the average of three biological replicates (p-value <0.05, +/- 1.2 fold change).

GENIE3 inferred network analysis

NanoString data from tissue grafting time course and from signalling experiments that did not use DMSO (i.e. lHM/BMP4 for 3 and 6 hours; FGF8 3 and 6 hours) were used to generate a predicted gene regulatory network. The mean expression values for each gene under each condition were analysed by the GENIE3 algorithm (Huynh-Thu et al., 2010). In brief, this algorithm decomposes n genes into n different regression problems. For each regression problem, the expression profile of one gene (target gene) is predicted from the expression profiles of all other genes (input genes), using tree-based ensemble methods. Within this the importance of a single input gene in explaining the profile of the target gene is assessed and an importance measure is generated. This importance measure is then used to predict the regulatory links and their direction within the network. Following analysis, interactions above an importance measure of 0.02 were isolated, based on the strength of their importance measure and the network was viewed using Cytoscape. For subsequent analysis genes of interest were highlighted with their first neighbours (putative regulators and targets) and small networks were created. To identify more closely related genes, community clustering was performed using the GLay plugin in Cytoscape (Su et al., 2010).

Acknowledgments

The authors are grateful to Ewa Kolano for excellent technical assistance, Ramya Ranganathan for *Cux1* in situ hybridisation in Fig. 2d' and Claudio D. Stern for comments on the manuscript and the Streit laboratory for discussions.

Competing Interests

The authors do not declare any competing interests.

Funding

This work was supported by the Diana Trebble studentship from the Dental Institute, a Studentship from Defeating Deafness UK (now Action on Hearing Loss) to AS and by project grants to AS from the NIH (DE022065) and the BBSRC (BB/I021647/1).

Data availability

Data were deposited in Gene Expression Omnibus (GSE48116, GSE81023).

Author Contributions

MH performed most experiments, analysed all data, generated the figures and contributed to writing the manuscript; RP performed the knockdown experiments, generated some figures and performed some in situ hybridizations for Figs. S2 and S3. MT performed in situ hybridisation of most genes, contributed to the FGF experiments and NanoString design; NC performed the experiments for the microarray screen; MA generated the GENIE3 network; TG was involved in the array analysis and the NanoString design. AS conceived the project, interpreted the data and wrote the manuscript.

References

Ahrens, K. and Schlosser, G. (2005). Tissues and signals involved in the induction of placodal Six1 expression in Xenopus laevis. *Dev Biol* **288**, 40-59.

Bailey, A. P., Bhattacharyya, S., Bronner-Fraser, M. and Streit, A. (2006). Lens specification is the ground state of all sensory placodes, from which FGF promotes olfactory identity. *Dev Cell* **11**, 505-517.

Bailey, A. P. and Streit, A. (2006). Sensory organs: making and breaking the pre-placodal region. In *Curr Top Dev Biol*, 167-204.

Baker, C. V. and Bronner-Fraser, M. (2001). Vertebrate cranial placodes I. Embryonic induction. *Dev Biol* **232**, 1-61.

Bally-Cuif, L., Gulisano, M., Broccoli, V. and Boncinelli, E. (1995). C-Otx2 Is Expressed in Two Different Phases of Gastrulation and Is Sensitive To Retinoic Acid Treatment in Chick Embryo. *Mech Dev* **49**, 49-63.

Bhat, N., Kwon, H.-J. and Riley, B. B. (2013). A gene network that coordinates preplacodal competence and neural crest specification in zebrafish. *Dev Biol* **373**, 107-117.

Brugmann, S. A., Pandur, P. D., Kenyon, K. L., Pignoni, F. and Moody, S. A. (2004). Six1 promotes a placodal fate within the lateral neurogenic ectoderm by functioning as both a transcriptional activator and repressor. *Development* **131**, 5871-5881.

Chambers, D. and Lumsden, A. (2009). Profiling Gene Transcription in the Developing Embryo. (ed. P. Sharpe & I. Mason), pp. 631-655: Humana Press.

Chen, B., Kim, E.-H. and Xu, P.-X. (2009). Initiation of olfactory placode development and neurogenesis is blocked in mice lacking both Six1 and Six4. *Dev Biol* **326**, 75-85.

Christophorou, N. A., Bailey, A. P., Hanson, S. and Streit, A. (2009). Activation of Six1 target genes is required for sensory placode formation. *Dev Biol* **336**, 327-336.

Dale, J. K., Vesque, C., Lints, T. J., Sampath, T. K., Furley, A., Dodd, J. and Placzek, M. (1997). Cooperation of BMP7 and SHH in the induction of forebrain ventral midline cells by prechordal mesoderm. *Cell* **90**, 257-269.

Delaune, E., Lemaire, P. and Kodjabachian, L. (2005). Neural induction in Xenopus requires early FGF signalling in addition to BMP inhibition. *Development* **132**, 299-310.

Dutta, S., Dietrich, J.-E., Aspöck, G., Burdine, R. D., Schier, A., Westerfield, M. and Varga, Z. M. (2005). Pitx3 Defines an Equivalence Domain for Lens and Anterior Pituitary Placode. *Development* **132**, 1579-1590.

Goriely, A., Diez del Corral, R. and Storey, K. G. (1999). c-Irx2 expression reveals an early subdivision of the neural plate in the chick embryo. *Mech Dev* **87**, 203-206.

Grocott, T., Johnson, S., Bailey, A. P. and Streit, A. (2011). Neural crest cells organize the eye via TGF-β and canonical Wnt signalling. *Nat Comm* **2**, 265-265.

Grocott, T., Tambalo, M. and Streit, A. (2012). The peripheral sensory nervous system in the vertebrate head: a gene regulatory perspective. *Dev Biol* **370**, 3-23.

Hamburger, V. and Hamilton, H. L. (1951). A series of normal stages in the development of the chick embryo. *J Morphol* **88**, 49-92.

Henry, J. J. and Grainger, R. M. (1990). Early tissue interactions leading to embryonic lens formation in Xenopus laevis. *Dev Biol* **141**, 149-163.

Holtfreter, J. (1933a). Der Einfluss von Wirtsalter und verschiedenen Organbezirken auf die Differenzierung von angelagertem Gastrulaektoderm. *Roux's Arch EntwMech* **127**, 619-775.

Holtfreter, J. (1933b). Eigenschaften und Verbreitung induzierender Stoffe. *Naturwissenschaften* **21**, 766-770.

Huynh-Thu, V. A., Irrthum, A., Wehenkel, L. and Geurts, P. (2010). Inferring regulatory networks from expression data using tree-based methods. *PLoS ONE* **5**.

Jacobson, A. G. (1963a). The determination and positioning of the nose, lens, and ear. I. Interactions within the ectoderm, and between the ectoderm and underlying tissues. *J Exp Zool* **154**, 273-283.

Jacobson, A. G. (1963b). The determination and positioning of the nose, lens, and ear. II. The role of the endoderm. *J Exp Zool* **154**, 285-291.
Khatri, S. B., Edlund, R. K. and Groves, A. K. (2014). Foxi3 is necessary for the induction of the chick otic placode in response to FGF signaling. *Dev Biol* **391**, 158-169.
Khudyakov, J. and Bronner-Fraser, M. (2009). Comprehensive spatiotemporal analysis of early chick neural crest network genes. *Dev Dyn* **238**, 716-723.
Kwon, H. J., Bhat, N., Sweet, E. M., Cornell, R. A. and Riley, B. B. (2010). Identification of early requirements for preplacodal ectoderm and sensory organ development. *PLoS Genet* **6**, e1001133.
Laclef, C., Souil, E., Demignon, J. and Maire, P. (2003). Thymus, kidney and craniofacial abnormalities in Six 1 deficient mice. *Mech Dev* **120**, 669-679.
Linker, C. and Stern, C. D. (2004). Neural induction requires BMP inhibition only as a late step, and involves signals other than FGF and Wnt antagonists. *Development* **131**, 5671-5681.
Litsiou, A., Hanson, S. and Streit, A. (2005). A balance of FGF, BMP and WNT signalling positions the future placode territory in the head. *Development* **132**, 4051-4062.
Lleras-Forero, L., Tambalo, M., Christophorou, N., Chambers, D., Houart, C. and Streit, A. (2013). Neuropeptides: developmental signals in placode progenitor formation. *Dev Cell* **26**, 195-203.
Mangold, O. (1933). Über die Induktionsfähigkeit der verschiedenen Bezirke der Neurula von Urodelen. *Naturwissenschaften* **21**, 761-766.
Monsoro-Burq, A. H., Fletcher, R. B. and Harland, R. M. (2003). Neural crest induction by paraxial mesoderm in Xenopus embryos requires FGF signals. *Development* **130**, 3111-3124.
New, D. A. T. (1955). A new technique for the cultivation of the chick embryo in vitro. *J Embryol Exp Morph* **3**, 326-331.
Nieuwkoop, P. D. and Nigtevecht, G. V. (1954). Neural activation and transformation in explants of competent ectoderm under the influence of fragments of anterior notochord in Urodeles. *J Embryol Exp Morph* **2**, 175-193.
Paxton, C. N., Bleyl, S. B., Chapman, S. C. and Schoenwolf, G. C. (2010). Identification of differentially expressed genes in early inner ear development. *Gene Expr Patterns* **10**, 31-43.
Pieper, M., Ahrens, K., Rink, E., Peter, A. and Schlosser, G. (2012). Differential distribution of competence for panplacodal and neural crest induction to non-neural and neural ectoderm. *Development* **139**, 1175-1187.
Qiao, Y., Zhu, Y., Sheng, N., Chen, J., Tao, R., Zhu, Q., Zhang, T., Qian, C. and Jing, N. (2012). AP2[gamma] regulates neural and epidermal development downstream of the BMP pathway at early stages of ectodermal patterning. *Cell Res* **22**, 1546-1561.
Rex, M., Orme, A., Uwanogho, D., Tointon, K., Wigmore, P. M., Sharpe, P. T. and Scotting, P. J. (1997). Dynamic expression of chicken Sox2 and Sox3 genes in ectoderm induced to form neural tissue. *Dev Dyn* **209**, 323-332.
Sato, S., Ikeda, K., Shioi, G., Ochi, H., Ogino, H., Yajima, H. and Kawakami, K. (2010). Conserved expression of mouse Six1 in the pre-placodal region (PPR) and identification of an enhancer for the rostral PPR. *Dev Biol* **344**, 158-171.
Saxen, L. and Toivonen, S. (1962). *Primary Embryonic Induction*. London: Logos/Academic.
Schlosser, G. (2010). Making senses development of vertebrate cranial placodes. *Int Rev Cell Mol Biol* **283**, 129-234.
Spemann, H. (1938). *Embryonic Development and Induction*. New Haven: Yale University Press.
Stern, C. D. (2001). Initial patterning of the central nervous system: how many organizers? *Nat Rev Neurosci* **2**, 92-98.
Stern, C. D. and Ireland, G. W. (1981). An integrated experimental study of endoderm formation in avian embryos. *Anat Embryol* **163**, 245-263.
Steventon, B., Mayor, R. and Streit, A. (2012). Mutual repression between Gbx2 and Otx2 in sensory placodes reveals a general mechanism for ectodermal patterning. *Dev Biol* **367**, 55-65.

Streit, A. (2008). The cranial sensory nervous system: specification of sensory progenitors and placodes. *StemBook*, 1-20.

Streit, A., Berliner, A. J., Papanayotou, C., Sirulnik, A. and Stern, C. D. (2000). Initiation of neural induction by FGF signalling before gastrulation. *Nature* **406**, 74-78.

Streit, A. and Stern, C. D. (2001). Combined whole-mount in situ hybridization and immunohistochemistry in avian embryos. *Methods* **23**, 339-344.

Stuhlmiller, T. J. and García-Castro, M. I. (2012). FGF/MAPK signaling is required in the gastrula epiblast for avian neural crest induction. *Development* **139**, 289-300.

Su, G., Kuchinsky, A., Morris, J. H., States, D. J. and Meng, F. (2010). GLay: community structure analysis of biological networks. *Bioinformatics* **26**, 3135-3137.

Takemoto, T., Uchikawa, M., Kamachi, Y. and Kondoh, H. (2006). Convergence of Wnt and FGF signals in the genesis of posterior neural plate through activation of the Sox2 enhancer N-1. *Development* **133**, 297-306.

Villanueva, S., Glavic, A., Ruiz, P. and Mayor, R. (2002). Posteriorization by FGF, Wnt, and retinoic acid is required for neural crest induction. *Dev Biol* **241**, 289-301.

Waddington, C. H. and Needham, J. (1936). Evocation, individuation, and competence in amphibian organizer action. *Proc Kon Akad Wetensch Amsterdam* **39**, 887-891.

Wilson, S. I., Graziano, E., Harland, R., Jessell, T. M. and Edlund, T. (2000). An early requirement for FGF signalling in the acquisition of neural cell fate in the chick embryo. *Curr Biol* **10**, 421-429.

Wilson, S. W. and Houart, C. (2004). Early steps in the development of the forebrain. *Dev Cell* **6**, 167-181.

Zheng, W., Huang, L., Wei, Z. B., Silvius, D., Tang, B. and Xu, P. X. (2003). The role of Six1 in mammalian auditory system development. *Development* **130**, 3989-4000.

Zou, D., Silvius, D., Fritzsch, B. and Xu, P. X. (2004). Eya1 and Six1 are essential for early steps of sensory neurogenesis in mammalian cranial placodes. *Development* **131**, 5561-5572.

Zou, D., Silvius, D., Rodrigo-Blomqvist, S., Enerback, S. and Xu, P.-X. (2006). Eya1 regulates the growth of otic epithelium and interacts with Pax2 during the development of all sensory areas in the inner ear. *Dev Bioly* **298**, 430-441.

Figures

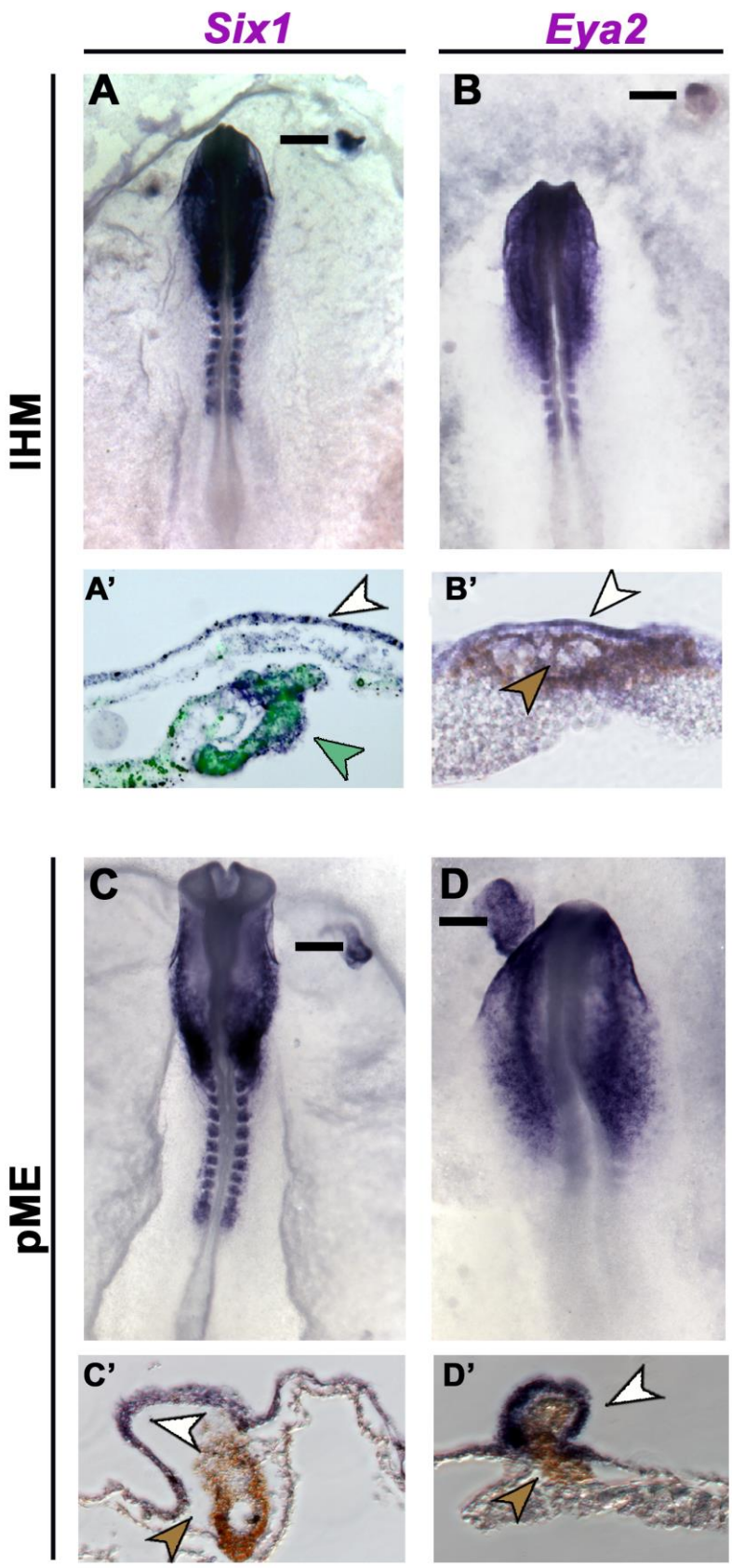

Figure 1. Induction of placode progenitors by the lateral head mesoderm and prechordal mesendoderm. A-B. CMFDA-labelled chick (green arrow in A') or quail (brown arrow in B') from HH5/6 donors induces *Six1* (A, A', white arrow; 8/8) and *Eya2* (B, B', white arrow; 3/10) in host extraembryonic epiblast. **C-D.** pME grafts from HH5/6 quail donors (brown) induce *Six1* (C, C'; 5/8) and *Eya2* (D, D'; blue; 7/8). Black lines in indicate section levels in A'-D'.

LHM (brown) induces *Six4* (B-b'; blue; 21/25) and *Eya2* after 12 hrs (C-c'; blue; 3/10).

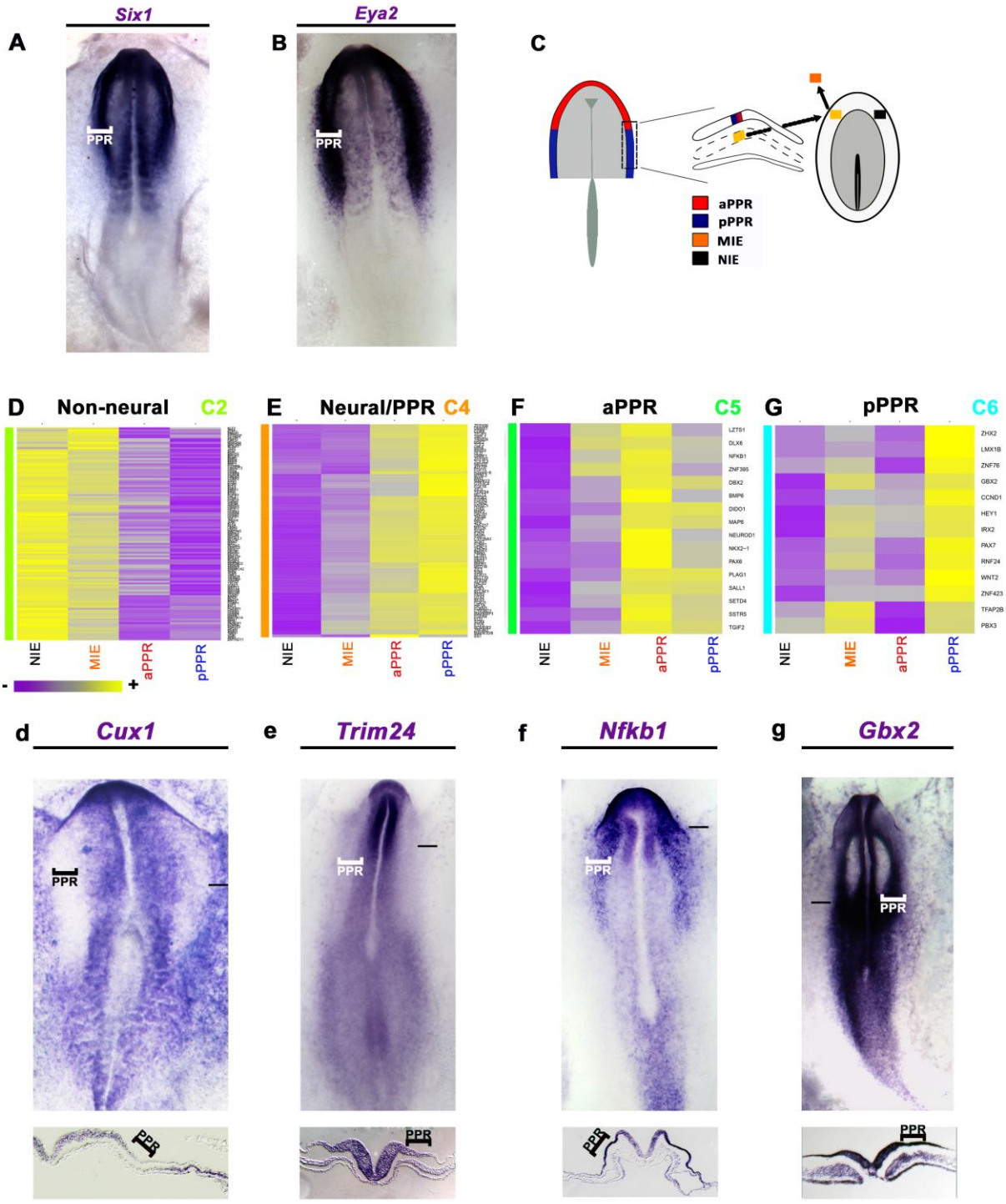

Figure 2. New placode progenitor transcripts. A-B. *Six1* (A) and Eya2 (B) expression at HH7^{+}/8^{-} (PPR: bracket). **C.** aPPR (red) and pPPR (dark blue) from HH6 (Lleras-Forero et al., 2013), mesoderm-induced (orange; MIE) and non-induced ectoderm (NIE: black) was analysed by microarray. **D.** Cluster C2 (light green): transcripts excluded from the PPR like *Cux1* (d). **E.** Cluster C4 (orange): aPPR and pPPR-enriched factors like *Trim24* (e). **F.** Cluster C5 (green): aPPR factors like *Nfkb1* (f). **G.** Cluster C6 (light blue): pPPR factors like *Gbx2* (g). Brackets in A-B, d-g: PPR position, lines in d-g: level of sections below.

A

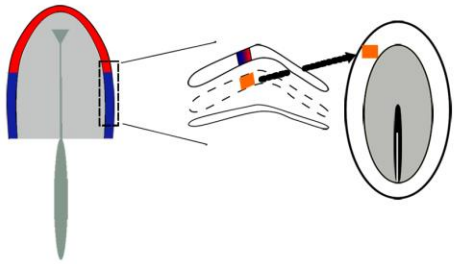

B

Gene	3hrs	6hrs	12hrs
Etv5			
Otx2			
ERNI			
Zic3			
Ccnd1			
N-myc			
Trim24			
Sall4			
Pdlim4			
Stox2			
Znf462			
Dnmt3b			
Irx2			
Rybp			
Dlx6			
Sall1			
Aatf			
Bcl7a			
Dach1			
Eya2			
Foxi3			
Gata3			
Gbx2			
Homer2			
pNoc			
Six1			
Six4			
Sox3			
Zhx2			
Axin2			
Bmp4			
Dlx3			
Dlx5			
Gata2			
Msx1			
Tfap2a			

Upregulated Downregulated

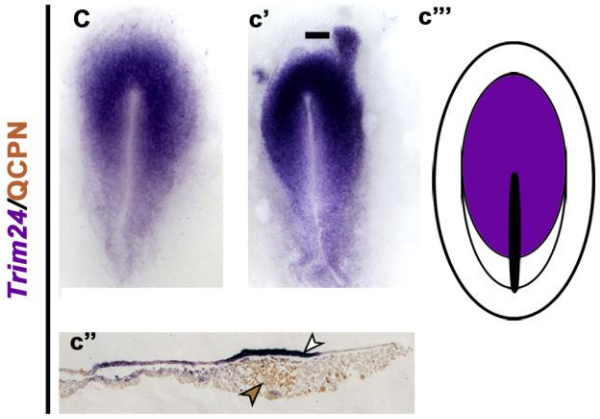

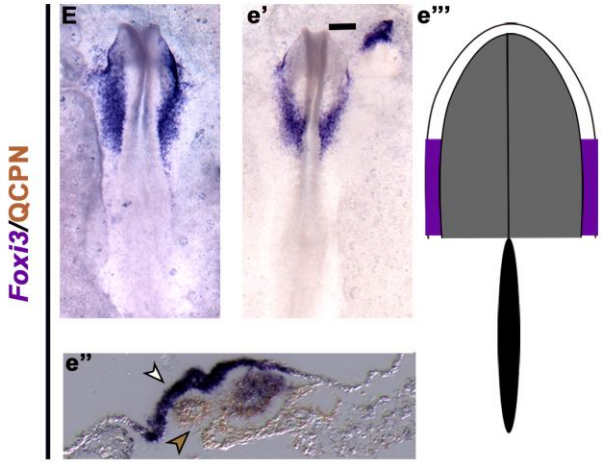

Figure 3. Response to the lateral head mesoderm. A. lHM (HH6; orange) was grafted into HH4^{-} hosts; the adjacent ectoderm was analysed after 3, 6 and 12 hours. **B.** Transcripts induced (yellow) or repressed (magenta) (p-value <0.05; fold-change > 1.2). **C-E**. Expression patterns of 3, 6 and 12 hour induced genes. c'-e', c''-e'': quail lHM (brown arrow in c''-e'') induces *Trim24* (c', c'' white arrow), *Dnmt3b* (d', d'' arrow head) and *Foxi3* (e', e'' arrow head). Black lines in c'-e' indicate the level of the sections shown in c''- e''. c'''-e''': Area of overlap (purple) of 3 (c'''), 6 (d''') and 12 hour (e''') -induced transcripts.

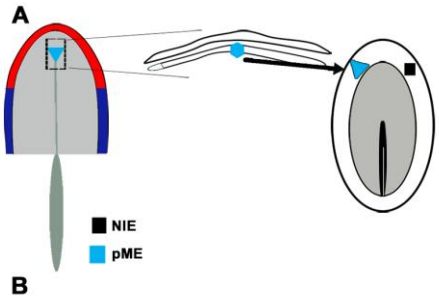

B

Gene	3hrs	6hrs	12hrs
Ccnd1			
ERNI			
Etv5			
N-myc			
Otx2			
Zic3			
Trim24			
Dmnt3b			
Eya2			
Hesx1			
Hey1			
Homer2			
Hsf2			
Irx2			
Sall1			
Six1			
Sox2			
Stox2			
Zic2			
Znf423			
Znf462			
Irx1			
Cited2			
Sox3			
Sstr5			
Bcl7a			
Dach1			
Dbx2			
Dlx6			
Ezh2			
Foxm1			
Gata3			
Hif1a			
Lmx1b			
Mier1			
Mynn			
Pdlim4			
pNOC			
Rybp			
Six3			
Zhx2			
Zic1			
Tfap2a			
Axin2			
Dlx3			
Gata2			
Dlx5			
Msx1			

Upregulated Downregulated

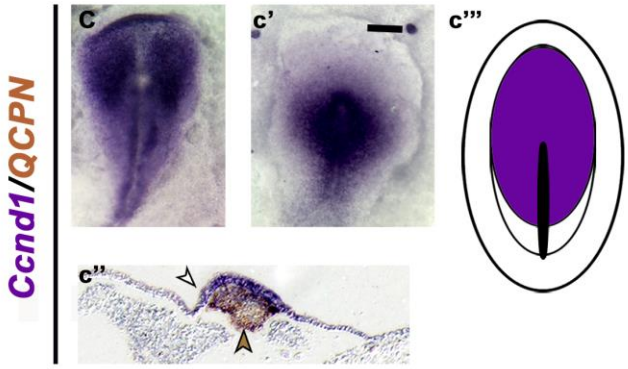

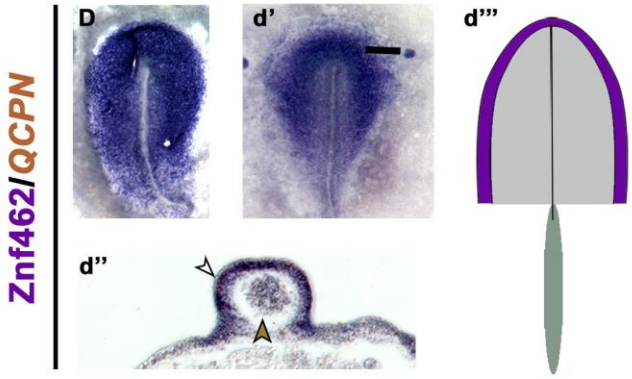

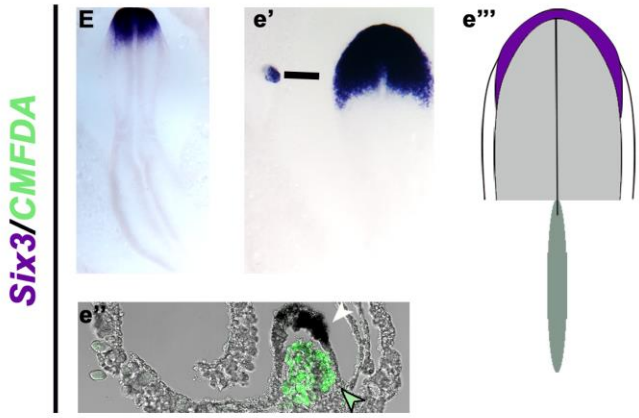

Figure 4. R**esponse to the prechordal mesendoderm. A.** pME (HH6; cyan) was grafted into HH4^{-} hosts; the adjacent ectoderm was analysed after 3, 6 and 12 hours. **B.** Transcripts induced (yellow) or repressed (magenta) (p-value <0.05; fold-change > 1.2). **C-E**. Expression patterns of 3, 6 and 12 hour induced genes. c'-e', c''-e'': quail pME (brown; arrow head in c''-d''; CMFDA: green; arrow head in e'') induces *Ccnd1* (c', c'' arrow head), *Znf462* (d', d'' arrow head) and *Six3* (e', e'' arrow head). Black lines in c'-e' indicate the level of the sections shown in c''- e''. c'''-e''': Area of overlap (purple) of 3 (c'''), 6 (d''') and 12 hour (e''') -induced transcripts.

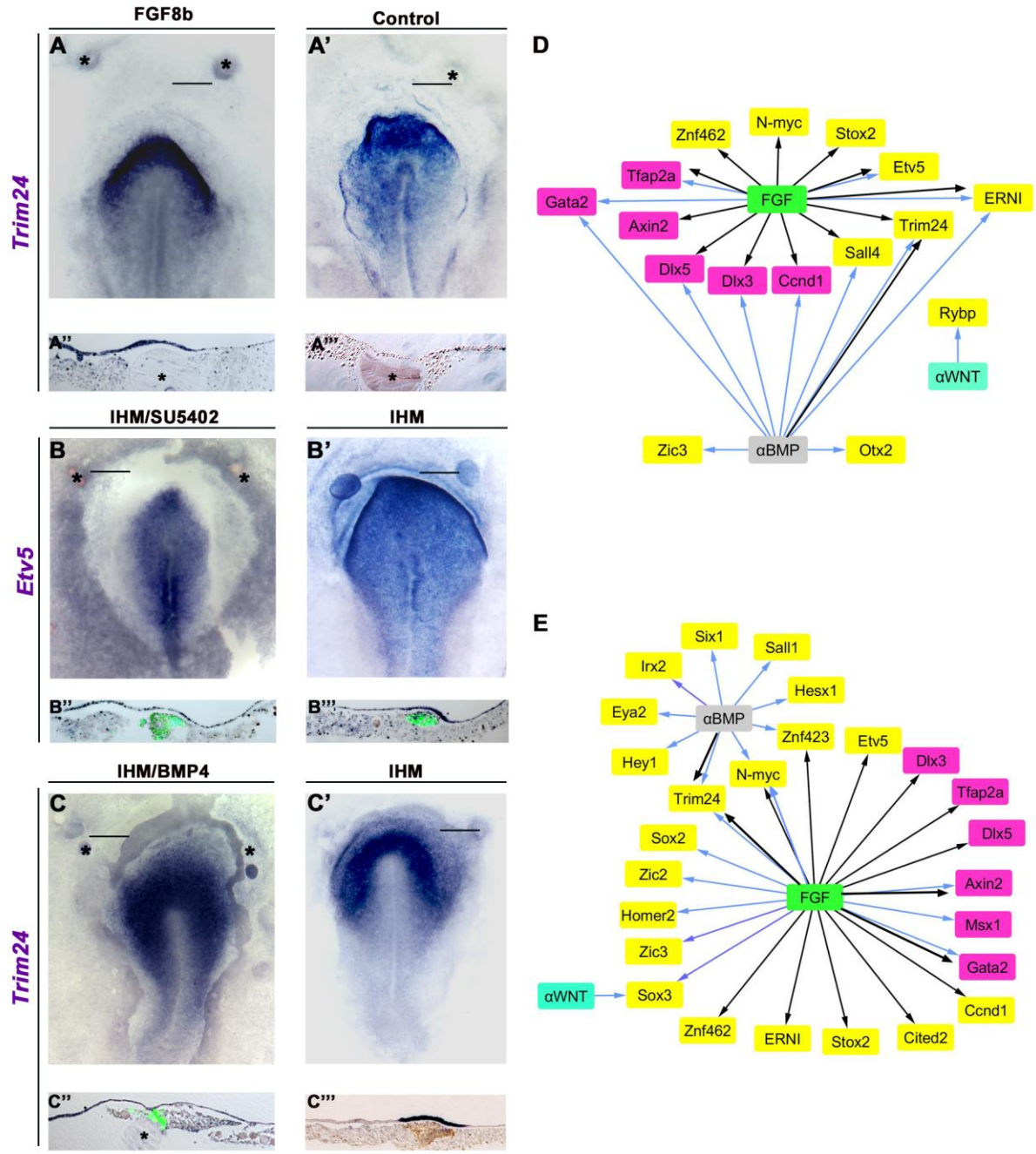

Figure 5. Signals controlling mesoderm response genes. A-A'''. Fgf8-coated (A, A''), but not control beads (A', A'''), induce *Trim24* after 3hrs (4/4). **B-B'''**. FGF signalling is required for the induction of *Etv5* by lHM. lHM (green in B'', B''') induces *Etv5* in extraembryonic epiblast (B', B'''; * control bead; 5/6); this is inhibited in the presence of SU5402-coated beads (* in B, B'' 4/4). **C-C'''**. *Trim24* is induced by lHM grafts (C', brown in C'''3/3); induction is inhibited in the presence of BMP4-coated beads (* in C, C''4/4). **D-E**. Different lHM (**D**) and pME (E) induced (yellow) or repressed (magenta)

genes respond to modulation of FGF (green), BMP (BMP antagonist: αBMP, grey) or Wnt (Wnt antagonist: αWNT; light blue). Black arrows: signal is sufficient; blue arrows: signal is required; see Table S4 and Fig. S7.

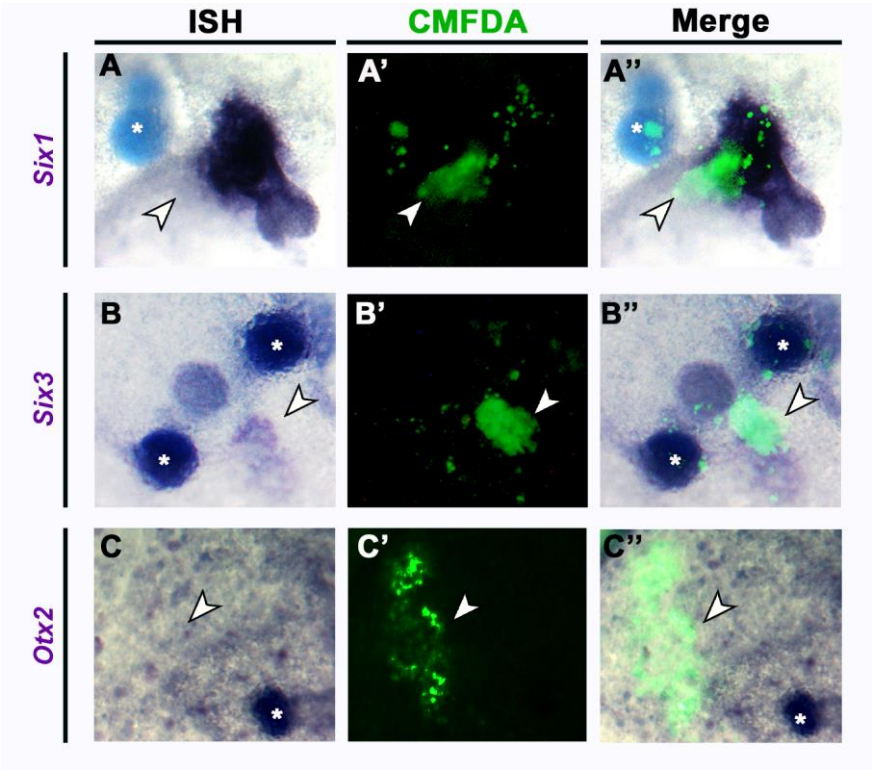

Figure 6. Sonic hedgehog is required for aPPR induction. CMFDA-labelled pME was grafted together with cyclopamine-coated beads into the extraembryonic region of chick hosts. After 16 hrs, *Six1* (**A-A''**) is induced (n=7/9 induced; no significant difference to controls, goodness of fit test). In contrast, *Six3* (**B-B''**; 4/13 induced; p-value = 0.00166, goodness of fit test; compared to 8/11 in controls, see Fig. 4e') and *Otx2* (0/4 induced; p-value = 0.024 (two-tailed) goodness of fit test; compared 3/3 in controls, see Fig. S11) induction is lost. Arrow heads: grafts. A-C in situ hybridisation, A'-C' green fluorescent grafts, A''-C'' overlay.

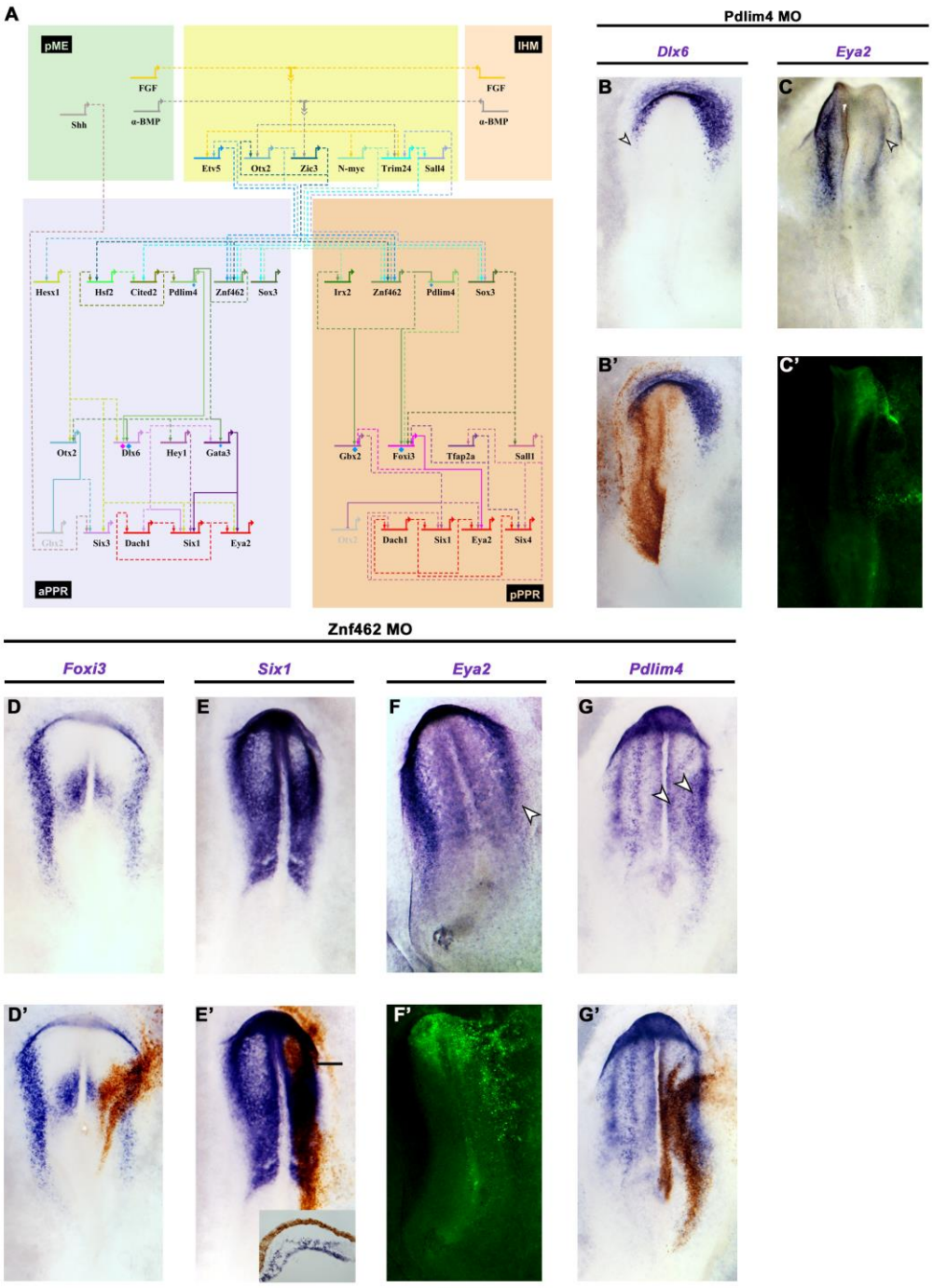

Figure 7. A predicted gene network reveals new candidate *Six1* and *Eya2* regulators. A. BioTapestry network integrating time series of transcript induction and interactions predicted from GENIE3. Genes induced after 3hrs: blue, 6hrs: green, 12hrs: purple; PPR genes: red. Dashed lines: predicted interactions; solid lines: known interactions and those experimentally verified in this study (blue diamonds for Znf462; pink diamonds for Pdlim4). **B-C'**. Pdlim4 knock down results in reduction of

Dlx6 (B, B': 5/5, brown MOs) and *Eya2* (C, C': 3/6, fluorescent MOs). **D-G**. Znf462 knock down leads to reduction of *Foxi3* (D, D': 4/5, brown MOs), *Six1* (E, E': 4/5, fluorescent MOs), and *Eya2* (F, F': 4/6, brown MOs; inset: transverse section), but an expansion of *Pdlim4* into the neural plate (G arrows, G': 3/5, brown MOs).

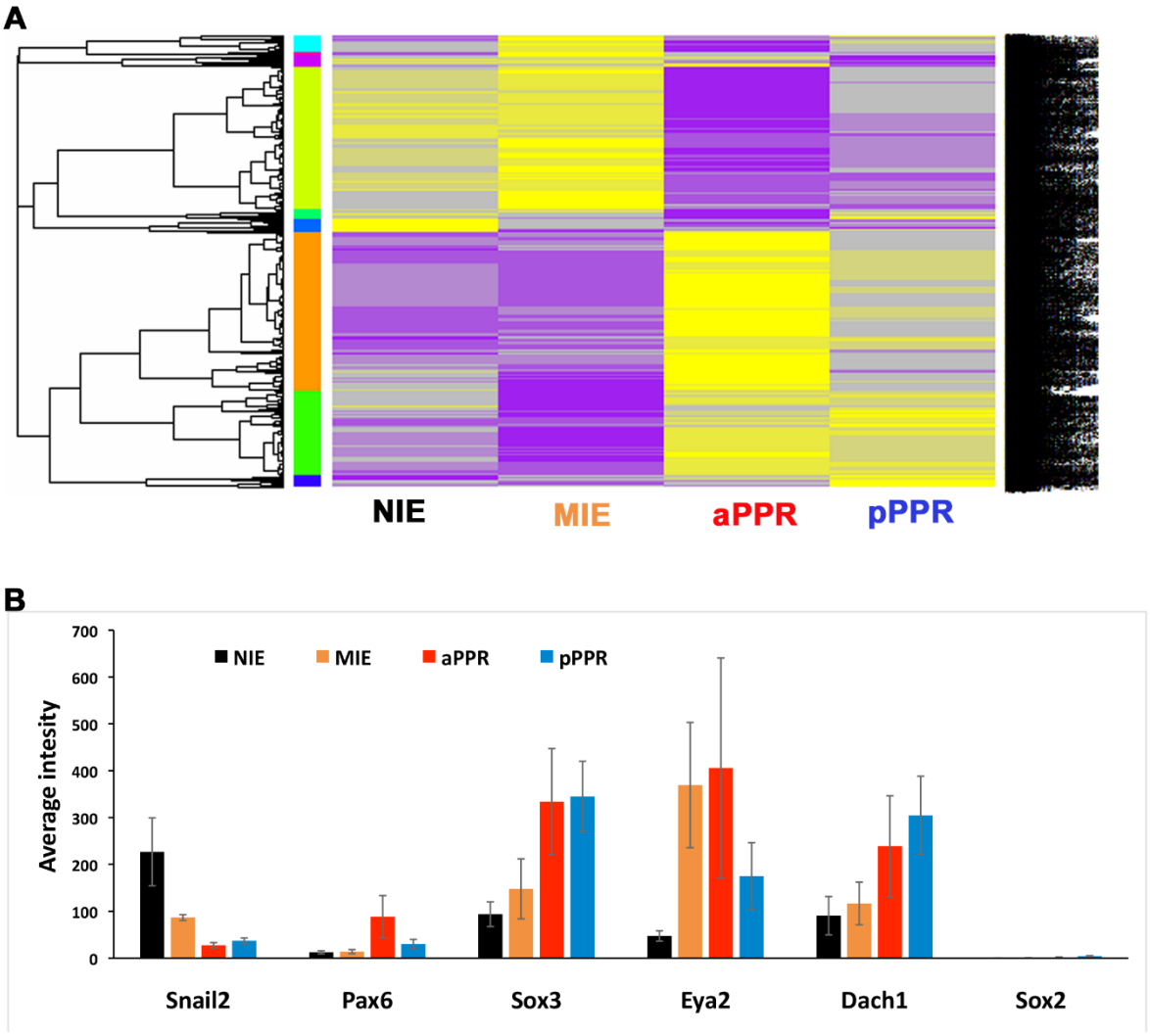

.

Figure S1. Analysis of microarray data. A. Hierarchical clustering of all transcripts shoeing significant changes in any of the four conditions. **B.** Bar graph shows the average gene intensity in the non-induced ectoderm (NIE), the mesoderm-induced ectoderm (MIE), the anterior pre-placodal region (aPPR) and posterior pre-placodal region (pPPR). Error bars represent SEM. These data replicate previous findings[27].

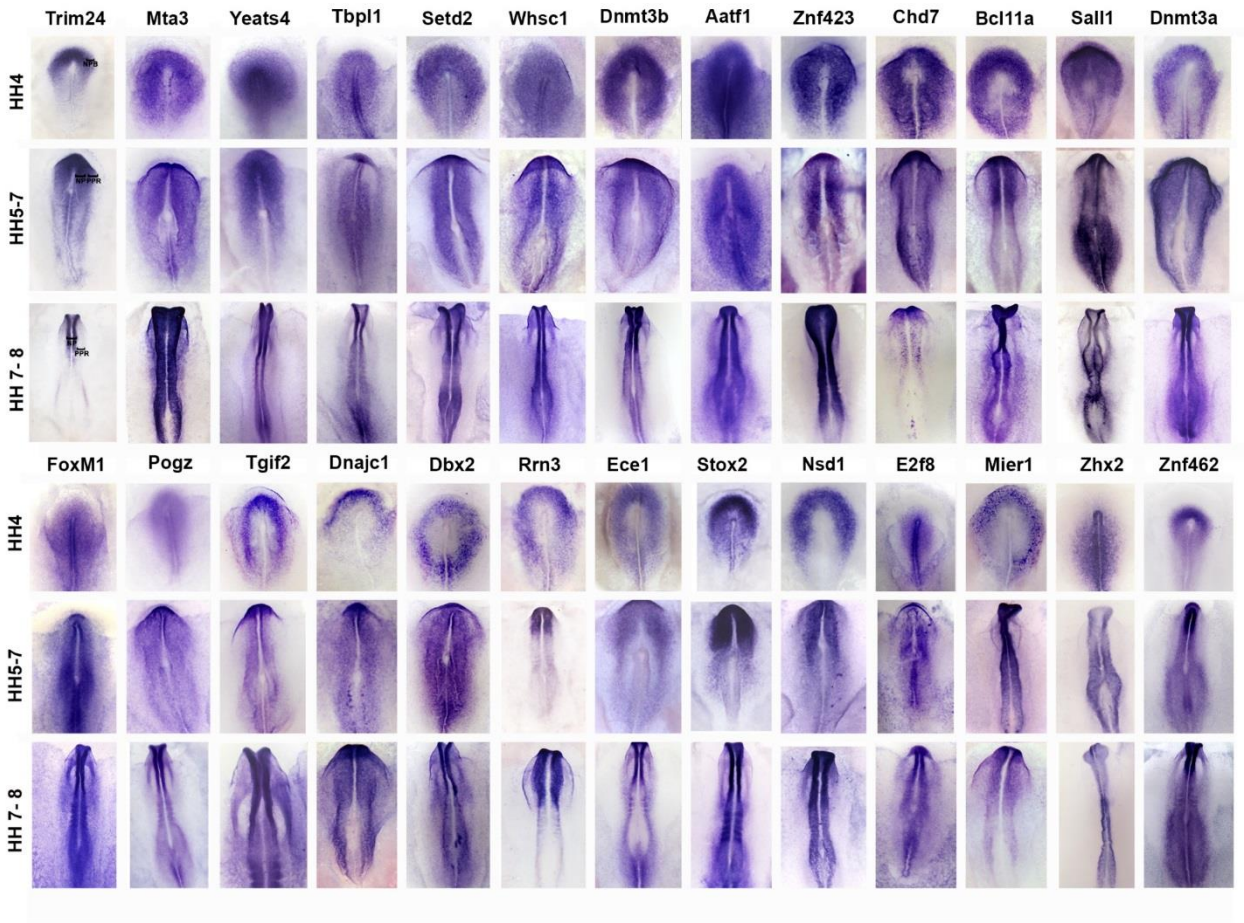

Figure S2. Expression patterns new factors identified by the microarray. In situ hybridisation shows gene expression at primitive streak (HH4), head fold (HH5-7) and early somite (HH8). NPB: neural plate border; NP: neural plate; PPR: pre-placodal region.

Figure S3 Expression patterns new factors identified by the microarray. In situ hybridisation shows gene expression at primitive streak (HH4), head fold (HH5-7) and early somite (HH8). NPB: neural plate border; NP: neural plate; PPR: pre-placodal region.

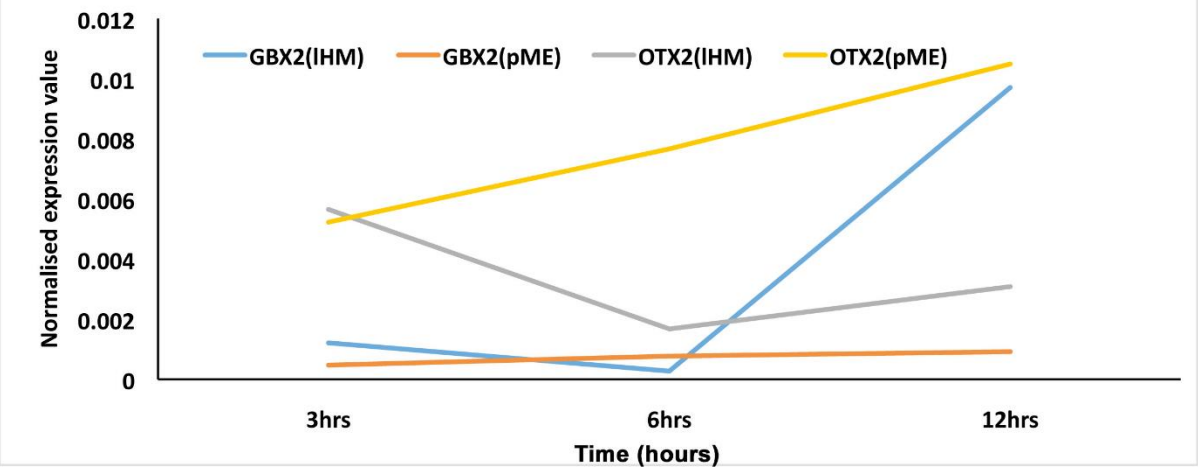

Figure S4. Changes in *Otx2* and *Gbx2* expression in response to the lateral head mesoderm and the prechordal mesendoderm. Line graph displaying the normalised expression values of *Otx2* and *Gbx2* at 3, 6 and 12 hours in response to both mesodermal tissues. Note: while *Gbx2* is strongly induced by the lateral head mesoderm (lHM; blue), the level of induction by the prechordal mesendoderm is extremely low (pME; dark orange). *Otx2* is induced by both tissues (pME: light orange; lHM: grey), but induction rapidly declines in response to lHM grafts.

IHM and pME induced genes after 3 hours

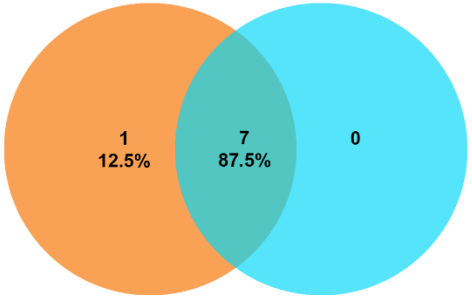

Sall4

Ccnd1
Erni
Etv5
N-myc
Otx2
Trim24
Zic3

(Gbx2)*
(Irx1)*
(SStr5)*

IHM and pME induced genes after 6 hours

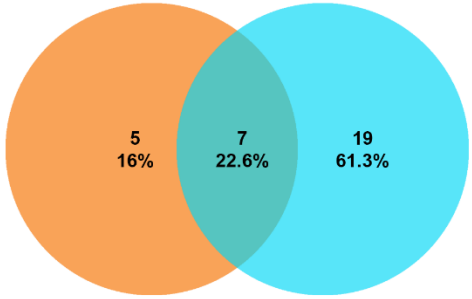

Cntnap5
Irx2
Pea3
Stox2
Rybp
Stox2

Dmnt3b
Erni
Etv5
Otx2
Setd2
Zic3
Znf462

Adnp2
ccnd1
Cited2
Dach1
Dnajc1
Geminin
Fsl4
Hsf2
Mef2d
Mynn
Nfkb1
N-myc
Sall1
Six1/4
Sox3
Trim24
Whsc1
Znf423

IHM and pME induced genes after 12 hours

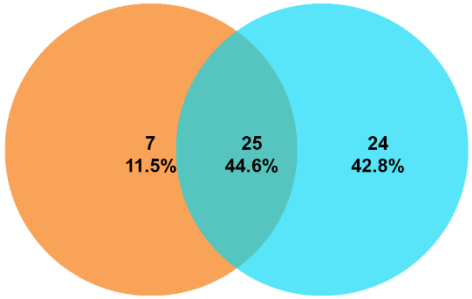

Aatf
Cxcl14
Foxi3
Six4
Sox3
Trim24
Whsc1

Bcl7a
Ccnd1
Cntnap5
Dach1
Dlx6
Dmnt3b
Etv5
Eya2
Fsl4
Gata3
Gbx2
Homer2
N-myc
Otx2
Pdlim4
pNOC
Sall1
Setd2
Six1
Stox2
Tbl1xr1
Tfap2a
Zhx2
Znf462

Chd7
Dbx2
Erni
Hey1
Hif1a
Hsf2
Irx1/2
Lmx1b
Mier1
Mynn
Pea3
Phf20
Six3
Sox2
Sp4
Sstr5
Tbx1
Zic1/2/3
Znf423

Figure S5. Comparison of the genes induced by the lateral head mesoderm and the prechordal mesendoderm. A. Venn diagram showing genes induced after 3, 6 and 12 hours. * these transcripts are induced, however since expression levels are extremely low were excluded from the analysis (see Figure S4).

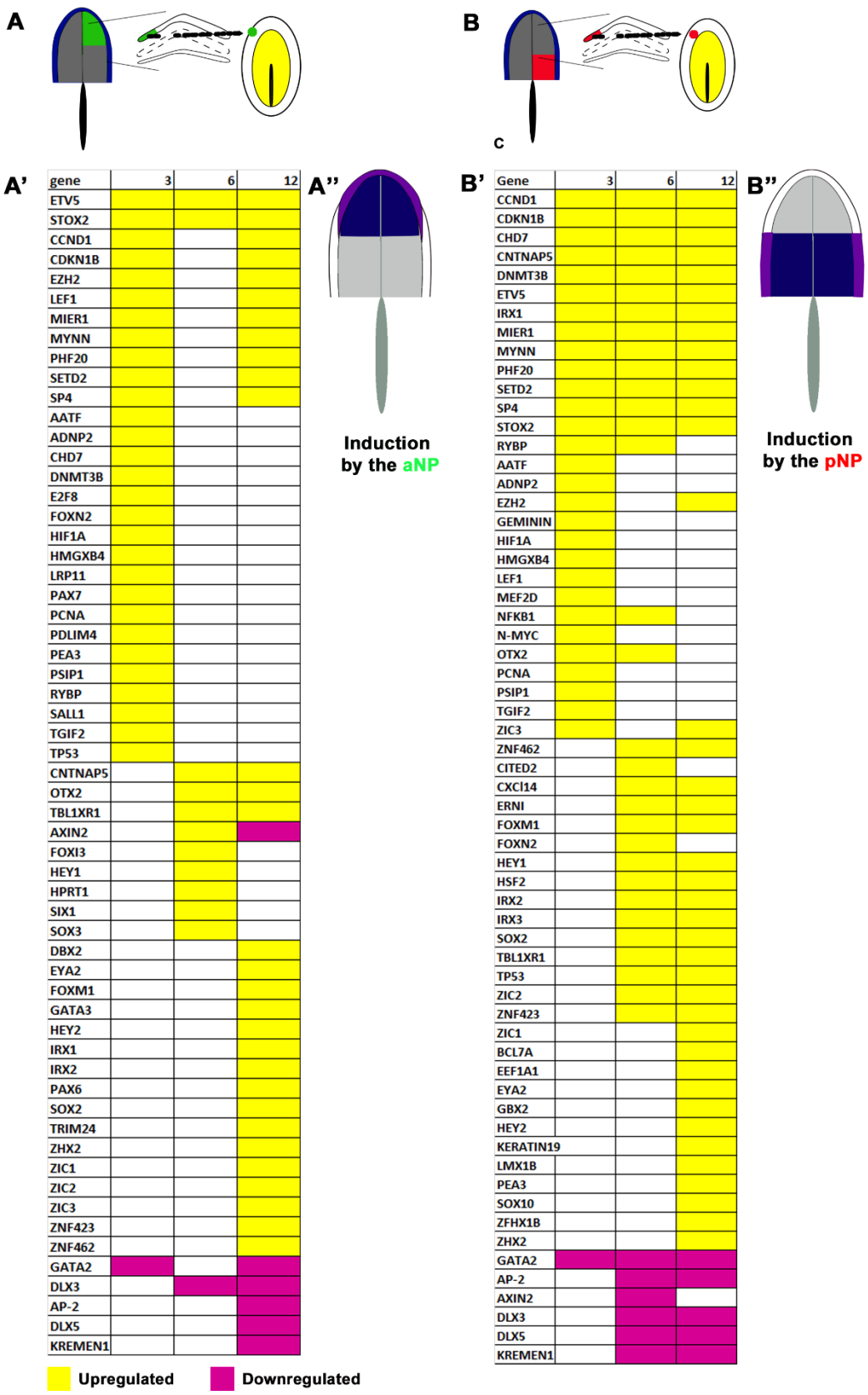

gene	3	6	12
ETV5			
STOX2			
CCND1			
CDKN1B			
EZH2			
LEF1			
MIER1			
MYNN			
PHF20			
SETD2			
SP4			
AATF			
ADNP2			
CHD7			
DNMT3B			
E2F8			
FOXN2			
HIF1A			
HMGXB4			
LRP11			
PAX7			
PCNA			
PDLIM4			
PEA3			
PSIP1			
RYBP			
SALL1			
TGIF2			
TP53			
CNTNAP5			
OTX2			
TBL1XR1			
AXIN2			
FOXI3			
HEY1			
HPRT1			
SIX1			
SOX3			
DBX2			
EYA2			
FOXM1			
GATA3			
HEY2			
IRX1			
IRX2			
PAX6			
SOX2			
TRIM24			
ZHX2			
ZIC1			
ZIC2			
ZIC3			
ZNF423			
ZNF462			
GATA2			
DLX3			
AP-2			
DLX5			
KREMEN1			

Gene	3	6	12
CCND1			
CDKN1B			
CHD7			
CNTNAP5			
DNMT3B			
ETV5			
IRX1			
MIER1			
MYNN			
PHF20			
SETD2			
SP4			
STOX2			
RYBP			
AATF			
ADNP2			
EZH2			
GEMININ			
HIF1A			
HMGXB4			
LEF1			
MEF2D			
NFKB1			
N-MYC			
OTX2			
PCNA			
PSIP1			
TGIF2			
ZIC3			
ZNF462			
CITED2			
CXCl14			
ERNI			
FOXM1			
FOXN2			
HEY1			
HSF2			
IRX2			
IRX3			
SOX2			
TBL1XR1			
TP53			
ZIC2			
ZNF423			
ZIC1			
BCL7A			
EEF1A1			
EYA2			
GBX2			
HEY2			
KERATIN19			
LMX1B			
PEA3			
SOX10			
ZFHX1B			
ZHX2			
GATA2			
AP-2			
AXIN2			
DLX3			
DLX5			
KREMEN1			

Figure S6. Genes regulated by the anterior and posterior neural plate. A, B. Experimental design. **A', B'.** Transcripts induced (yellow) or repressed (magenta) in the extraembryonic ectoderm by the anterior (aNP) or posterior neural plate (pNP) (p-value <0.05; fold-change > 1.2) 3, 6 and 12 hours after grafting. A'': genes induced by the aNP at 12 hours are normally expressed in the anterior neural plate, the anterior PPR or both. B'': genes induced by the pNP at12 hours are normally expressed in the posterior neural plate, the posterior PPR or both.

Signals mediating PPR induction by the lateral head mesoderm

3 hours

Gene	FGF8	lHM/SU	lHM/BIO	lHM/BMP4	Dorso
Etv5					
Trim24					
Ccnd1					
ERNI					
N-myc					
Sall4					
Otx2					
Zic3					
Dlx5					
Tfap2a					
Axin2					
Gata2					

6 hours

Gene	FGF8	lHM/SU	lHM/BIO	lHM/BMP4
Etv5				
Stox2				
Znf462				
ERNI				
Rybp				
IRX2				
OTX2				
ZIC3				
DLX5				
TFAP2a				
AXIN2				
GATA2				
DLX3				

Signals mediating PPR induction by the prechordal mesendoderm

3 hours

Gene	FGF8	pME/SU	pME/BIO	pME/BMP4	Dorso
Trim24					
N-myc					
Ccnd1					
ERNI					
Etv5					
Otx2					
Zic3					
Tfap2a					
Axin2					
Dlx3					
Dlx5					
Gata2					

Upregulated **Downregulated**

6 hours

Gene	FGF8	pME/SU	pME/BIO	pME/BMP4
N-myc				
Trim24				
Znf423				
Ccnd1				
Cited2				
Etv5				
Stox2				
Znf462				
Sox3				
Homer2				
Sox2				
Zic2				
Zic3				
Eya2				
Hesx1				
Hey1				
Irx2				
Sall1				
Six1				
ERNI				
Otx2				
Gata2				
Dlx3				
Dlx5				
Axin2				
Msx1				
Tfap2a				

Figure S7. Signalling factors mediating PPR induction by the mesoderm. FGF, BMP and Wnt signalling was modulated as described in the text. The behaviour of transcripts activated (green) or repressed (red) by the lateral head mesoderm (top) or the prechordal mesendoderm (bottom) were assessed for their response to different signals or tissue/factor combinations. Table shows up- (yellow) or downregulation (magenta) of a transcript compared to controls at 3 hours or 6 hours after each manipluation (p-value <0.05; fold-change > 1.2); no change is shown in white. FGF8: graft of FGF8 coated beads compared to control beads. lHM/SU: lateral head mesoderm + SU5402 coated beads compared to lateral head mesoderm + DMSO coated beads; pME/SU prechordal mesendoderm + SU5402 coated beads compared to prechordal mesendoderm + DMSO coated beads. lHM/BIO: lateral head mesoderm + BIO coated beads compared to lateral head mesoderm + DMSO coated beads; pME/BIO prechordal mesendoderm + BIO coated beads compared to prechordal mesendoderm + DMSO coated beads. lHM/BMP4: lateral head mesoderm + BMP4 coated beads compared to lateral head mesoderm + control beads; pME/BMP4 prechordal mesendoderm + BMP4 coated beads compared to prechordal mesendoderm + control beads. Dorso: Dorsomorphin treated extraembryonic ectoderm

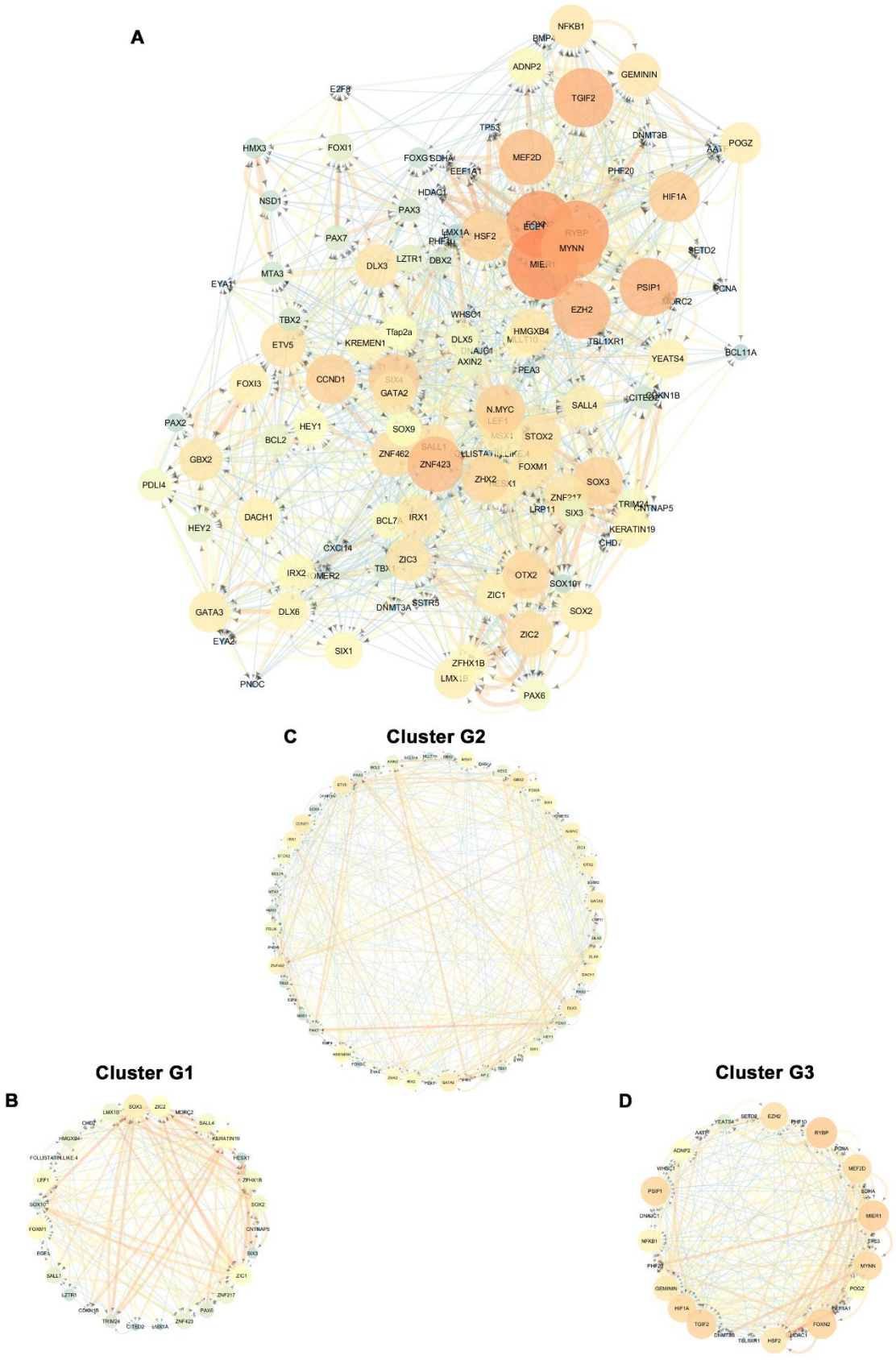

Figure S8. Predicted network modelling interactions during PPR induction. A. Interactions above importance measure of 0.02 from GENIE3 algorithm plotted in cytoscape. Nodes are size- and colour-coded according to their outdegree with large and red nodes having the highest outdegree, and small/blue the lowest. Edges indicating interactions are coded according to importance measure (high: thick lines; low: thin lines). **B-D.** The network segregates into three community clusters Cluster G1, G2 and G3.

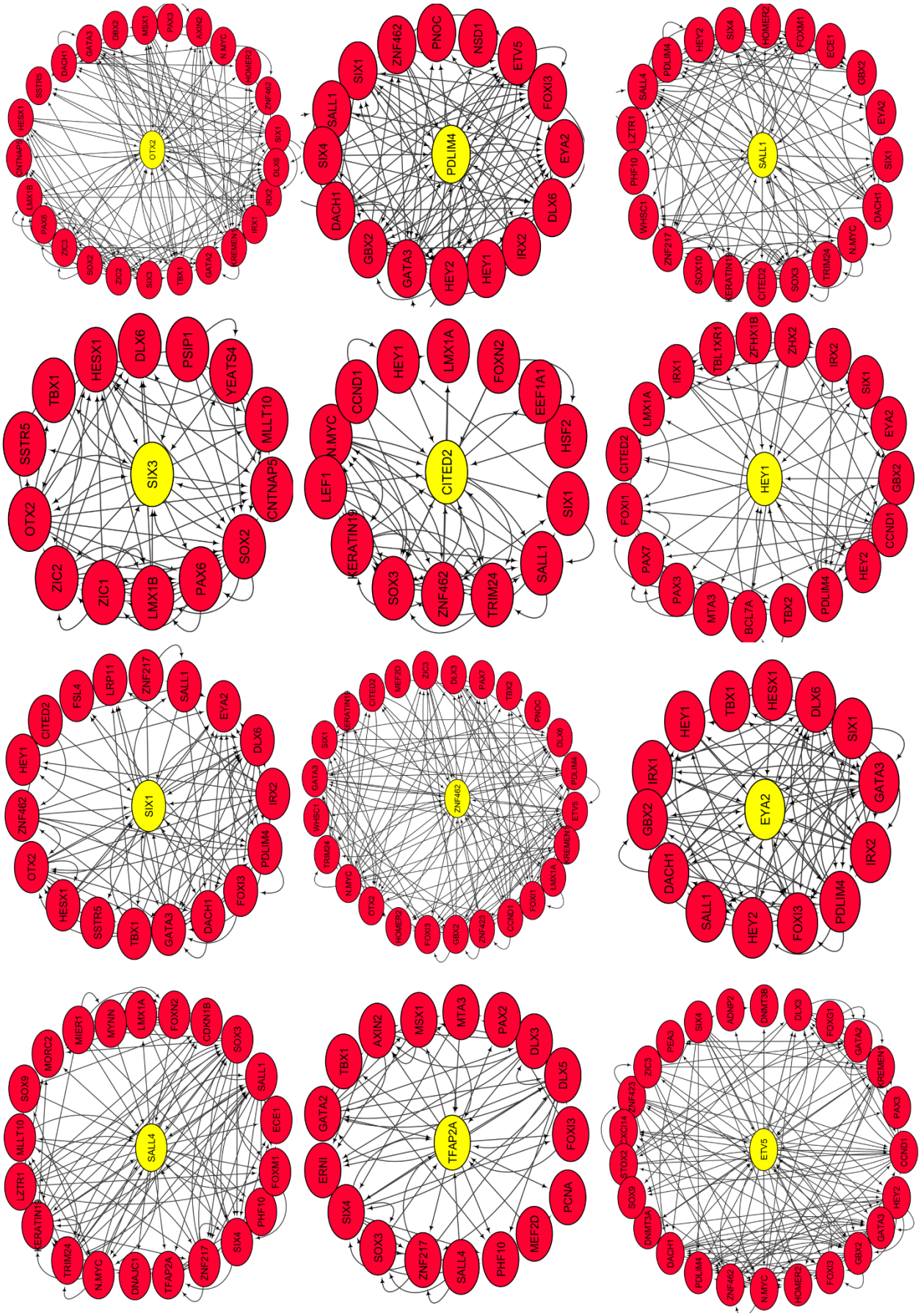
OTX2
PDLIM4
SALL1
SIX3
CITED2
HEY1
SIX1
ZNF462
TFAP2A
ETV5
EYA2
SALL4

Figure S9. Nearest neighbours of genes connected to Six1, Six4 and Eya2. Six1, Eya2 and genes present at 3 hours and 6 hours (yellow) were isolated from the GENIE3 network together with their first neighbours (red). Arrows indicate the predicted direction of regulation. These data were used to construct the BioTapestry network in Figure 7.

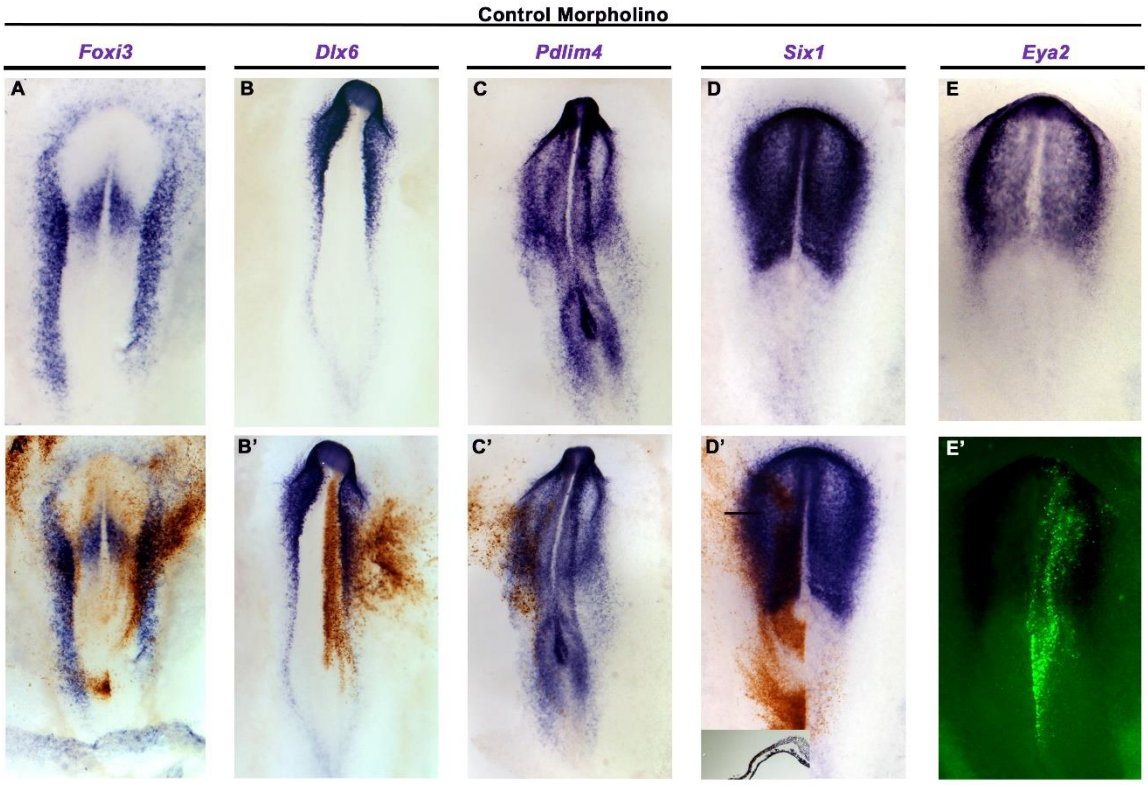

Figure S10: Electroporation of control morpholinos. Embryos were electroporated with control morpholino at HH4^{+} and assayed for *Foxi3* (A, A': brown MOs, 4/5 normal), *Dlx6* (B, B': brown MOs, 4/4 normal), *Pdlim4* (C, C': brown MOs, 4/4 normal), *Six1* (D, D': brown MOs, insert traverse section; 4/4 normal), *Eya2* (E, E': green fluorescent MOs, 6/6 normal).

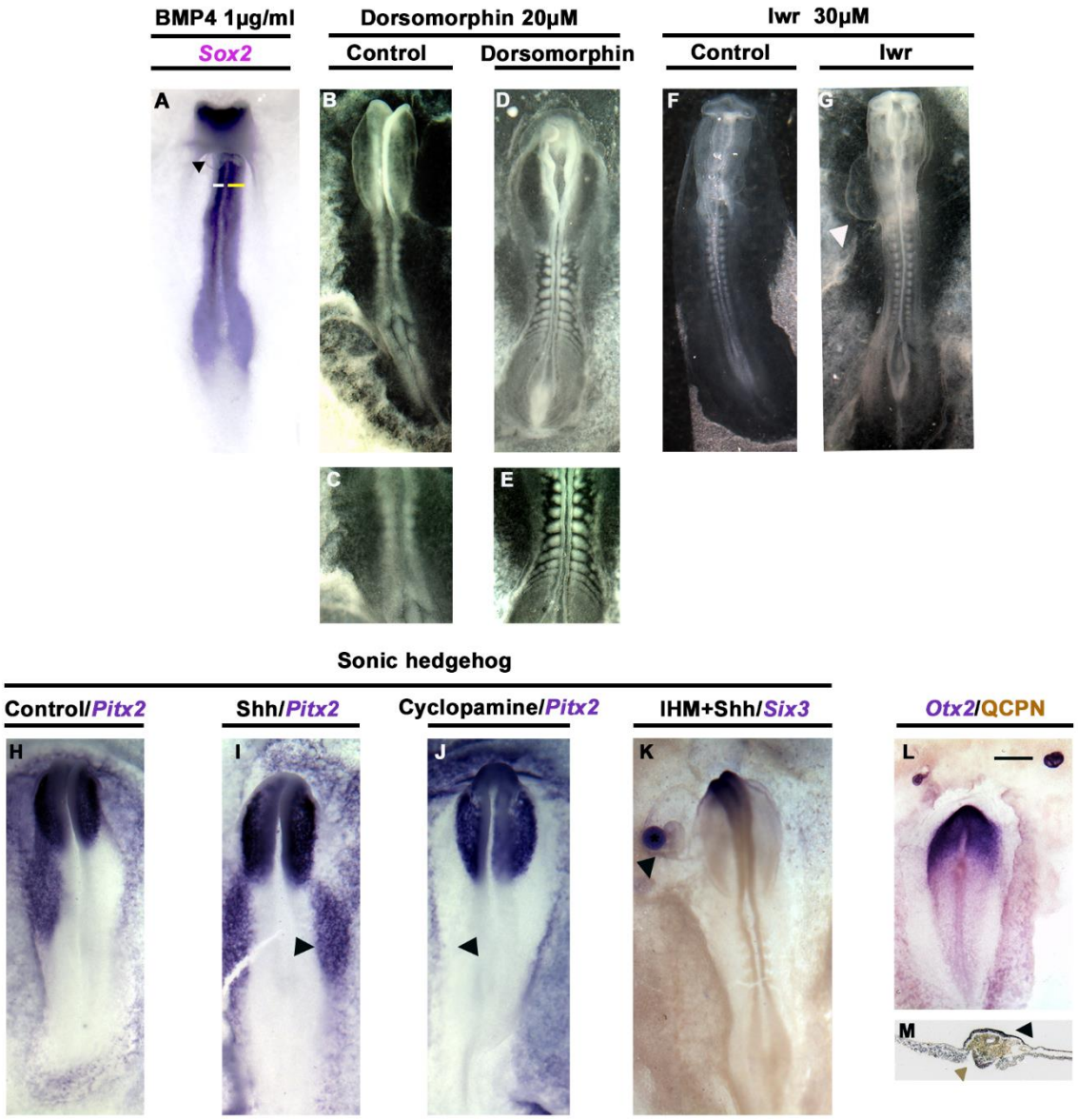

Figure S11: Positive controls for signalling experiments. A. The neural plate labelled by *Sox2* is narrowed in the presence of BMP4 coated beads (arrow head); compare by white bar on the experimental and yellow bar on the control side. **B-C**. Embryos grown in the presence of DMSO for 12 hours show normal somite development (n=5); E. increased magnification of somites. **D-E.** Embryos grown in the presence of the BMP antagonist Dorsomorphin (20µM) for 12 hours display expanded somites (n = 3); E. increased magnification of somites. **F.** Control embryos grown in the presence of DMSO show no heart defects. **G.** Embryos grown in the presence of 30µM IWR-1 display heart defects,

including enlarged or malformed hearts (n=9). **H.** *Pitx2* expression in the lateral plate mesoderm is confined to the left side in control embryos (n= 3). **I.** When grafted to the right side of the node, beads coated with 100µg/ml Shh induce symmetric *Pitx2* (black arrow, n = 2). **J.** Cyclopamine (1µM) coated beads grafted to the left side of the node lead to the loss of *Pitx2* (n = 3). **K.** lHM grafted together with Shh-coated beads do not induce anterior markers like *Six3*. **L-M.** pME grafts induce the expression of *Otx2* in host epiblast (3/3); black line indicates level of section shown in N. black arrow: *Otx2* expression, brown arrow: QCPN stained quail pME).

Supplementary Table 1. Microarray data. Transcripts showing significant changes of expression in at least one condition (sheet 1) and extracted transcription and signaling factors. The latter are labelled according to the clusters shown in Figure S1.

Click here to Download Table S1

Supplementary Table 2. List of the transcripts induced by the lHM >1.2 fold change or repressed <0.8 fold change, <0.05 P-value.

Click here to Download Table S2

Supplementary Table 3. Genes included on the NanoString probe set and their target sequence.

Click here to Download Table S3

Supplementary Table 4. Data for all NanoString experiments showing all statistically significant genes (Students 2 tailed t-test P-value <0.05).

Click here to Download Table S4

	Primitive streak stage			PPR stage			Placode stage (HH10-12)							References
Gene	neural plate	neural plate border	NNE	neural plate	PPR	NNE	neural tube	Lens	Otic	Trigeminal	OLP	NCC	NNE	
AATF1														Fig. S2
ADNP2														Trevers, 2015
AP-2a														Khudyakov and Bonner-Fraser, 2009
AXIN2														Trevers, 2015
BCL11A														Fig. S2
BCL2														
BCL7A														
BCLAF1														Fig. S3
BMP4							dNT							Streit and Stern, 1999; Bothe et al., 2011
CCND1														Fig. 2 and 3
CDKN1B														
CHD7														Fig. S2
CITED2				pNP										Schlange, 2000
CNTNAP5				w										Geisha.arizona.edu
CXCl14		p					HB		Rim					Alev, 2010; Chen et al., 2016
CXXC6-like				aNP	aPPR									Lleras-Forero, 2012
DACH1														Litsiou, 2005
DBX2														Fig. S2; Geisha.arizona.edu
DLX3														Khudyakov and Bonner-Fraser, 2009
DLX5														Streit, 2002; Brown et al., 2005
DLX6	w					w								Fig. S3; Brown et al., 2005
DMBX1					aPPR		MB							Fig. S3; Geisha.arizona.edu
DNAJC1														Fig. S2
DNMT3A														Fig. S2; Tambalo 2015; Hu et al., 2012a
DNMT3B														Fig. S2; Tambalo 2015; Hu et al., 2012b
E2F8														Fig. S2
ECE1														Fig. S2
EEF1A1							HB							Chambers et al., 2006
ERNI														Streit et al., 2000
ETV5														Lunn et al., 2007
EYA1				w										Ishihara et al., 2008
EYA2														McLarren et al., 2003; Ishihara et al., 2008
EZH2														Trevers, 2015
FOXG1	aNP			aNP			FB							Bell et al., 2001; Bailey et al., 2006; Chapman et al., 2008
FOXI2														Khatri et al, 2013
FOXI3					pPPR									Khatri et al, 2013
FOXM1					w									Fig. S2; Tambalo 2015
FOXN2														Fig. S3
FSL4	aNP			aNP	aPPR									Chapman et al., 2002; Chen et al., 2016
GATA2														Sheng and Stern, 1999;
GATA3														Sheng and Stern, 1999; Bothe and Dietrich, 2003
GBX2	pNP	p		pNP	pPPR									Niss and Leutz, 1998; Shamim and Mason, 1998; Paxton et al., 2010
GEMININ	w													Papanayotou et al., 2008
HESX1	aNP			aNP			FB							Chapman et al., 2003; Abe et al., 2006
HEY1														Geisha.arizona.edu
HEY2							HB							Geisha.arizona.edu
HMGXB4														Fig. S3; Tambalo 2015
HMX3														Herbrand et al, 1998
HOMER2														Fig. S3
HSF2					aPPR				w					Fig. S3; Tambalo 2015
ING5				pNP	aPPR									Fig. S3
IRX1														Khudyakov and Bonner-Fraser, 2009
IRX2														Geisha.arizona.edu
KERATIN19														McLarren et al., 2003; Geisha.arizona.edu
KREMEN1	pNP			pNP	pPPR									Llears-Forero, 2012
LEF1							MB, HB		pOP					Schmidt et al., 2004
LMX1A														Chen et al., 2016; Geisha.arizona.edu
LMX1B														Abello et al., 2010; Geisha.arizona.edu
LRP11	w			w	w									Fig. S3
LZTR1														Fig. S3
MIER1				aNP	aPPR w									Fig. S2
MLLT10														Fig. S3
MORC10														Fig. S3
MSX1														Streit, 2002
MTA3														Fig. S2
MYNN														Fig. S3; Tambalo 2015
NFKB1					aPPR									Fig. S3
N-MYC														Khudyakov and Bonner-Fraser, 2009
NSD1					aPPR									Fig. S2; Trevers, 2015
OTX2				aNP	aPPR		aNT							Plouhinec et al., 2005
PAX2							MHB							Groves and Bronner-Fraser, 2000; Streit, 2002
PAX3														Bothe et al., 2007; McCabe and Bronner-Fraser, 2008
PAX6					aPPR		FB							Bell et al., 2001; Bhattacharyya et al., 2004
PAX7														Basch et al., 2007; Khudyakov and Bonner-Fraser, 2009
PDLIM4														Fig. S3; Geisha.arizona.edu
PEA3														Lunn et al., 2007
PNOC					aPPR									Lleras-Forero et al., 2013
POGZ														Fig. S2
PSIP1														Fig. S3
RRN3														Fig. S2
RYBP														Fig.S3
SALL1														Fig. S2; Sweetman et al., 2005
SALL4													w	Barembaum and Bronner-Fraser, 2007; Geisha expression pattern
SETD2					w									Fig. S2; Tambalo 2015
SIX1	w													Litsiou et al., 2005; Sato et al., 2012
SIX3	aNP			aNP	aPPR		FB							Bovolenta et al., 1998
SIX4	w													Esteve and Bovolenta, 1999
SOX10														Cheng et al., 2000; McKeown et al., 2005; Geisha expression pattern
SOX2														Uchikawa et al., 2003
SOX3														Rex et al., 1997; Abu-Elmagd et al., 2001; Mikawa et al., 2004; Streit and Stern, 1999
SOX9														McKeown.2005
SP4														
SSTR5					aPPR									Lleras-Forero et al., 2013
STOX2														Fig. S2
TBL1XR1														Trevers, 2015
TBPl1														Fig. S2
TBX3														Trevers 2015
TGIF2														Fig. S2
TRIM24														Fig. S2
WHSC1														Fig. S2; Tambalo 2015
YEATS4														Fig. S2
ZFHX1B														Dady et al., 2012
ZHX2														Fig. S2
ZIC1							dHB							Khudyakov and Bonner-Fraser, 2009; Geisha expression pattern; Trevers, 2015
ZIC2														Trevers, 2015
ZIC3														McMahon et al., 2010; Trevers, 2015
ZNF217														Trevers, 2015
ZNF423														Fig. S2
ZNF462														Fig. S2

1. Abe, Y., Chen, W., Huang, W., Nishino, M. & Li, Y. P. CNBP regulates forebrain formation at organogenesis stage in chick embryos. *Dev. Biol.* **295,** 116–127 (2006)
2. Abelló, G. *et al.* Independent regulation of Sox3 and Lmx1b by FGF and BMP signaling influences the neurogenic and non-neurogenic domains in the chick otic placode. *Dev. Biol.* **339,** 166–178 (2010).
3. Abu-Elmagd, M. *et al.* cSox3 expression and neurogenesis in the epibranchial placodes. *Dev. Biol.* **237,** 258–269 (2001).
4. Alev, C. *et al.* Transcriptomic landscape of the primitive streak. *Development* **137,** 2863–2874 (2010).
5. Bailey, A. P., Bhattacharyya, S., Bronner-Fraser, M. & Streit, A. Lens specification is the ground state of all sensory placodes, from which FGF promotes olfactory identity. *Dev. Cell* **11,** 505–17 (2006).
6. Barembaum, M. & Bronner-Fraser, M. Spalt4 mediates invagination and otic placode gene expression in cranial ectoderm. *Development* **134,** 3805–14 (2007).
7. Basch, M. L., Bronner-Fraser, M. & García-Castro, M. I. Specification of the neural crest occurs during gastrulation and requires Pax7. *Nature* **441,** 218–222 (2006).
8. Bell, E., Ensini, M., Gulisano, M. & Lumsden, a. Dynamic domains of gene expression in the early avian forebrain. *Dev. Biol.* **236,** 76–88 (2001).
9. Bhattacharyya, S., Bailey, A. P., Bronner-Fraser, M. & Streit, A. Segregation of lens and olfactory precursors from a common territory: cell sorting and reciprocity of Dlx5 and Pax6 expression. *Dev. Biol.* **271,** 403–14 (2004).
10. Bothe, I. & Dietrich, S. The molecular setup of the avian head mesoderm and its implication for craniofacial myogenesis. *Dev. Dyn.* **235,** 2845–2860 (2006).
11. Bothe, I., Tenin, G., Oseni, A. & Dietrich, S. Dynamic control of head mesoderm patterning. *Development* **138,** 2807–21 (2011).
12. Bovolenta, P., Mallamaci, A., Puelles, L. & Boncinelli, E. Expression pattern of cSix3, a member of the Six/sine oculis family of transcription factors. *Mech. Dev.* **70,** 201–203 (1998).
13. Brown, S. T., Wang, J. & Groves, A. K. Dlx gene expression during chick inner ear development. *J. Comp. Neurol.* **483,** 48–65 (2005).
14. Chambers, D. & Mason, I. Expression of sprouty2 during early development of the chick embryo is coincident with known sites of FGF signalling. *Mech. Dev.* **91,** 361–364 (2000).
15. Chapman, S. C., Schubert, F. R., Schoenwolf, G. C. & Lumsden, A. Analysis of spatial and temporal gene expression patterns in blastula and gastrula stage chick embryos. *Dev. Biol.* **245,** 187–199 (2002).
16. Chapman, S. C., Schubert, F. R., Schoenwolf, G. C. & Lumsden, A. Anterior identity is established in chick epiblast by hypoblast and anterior definitive endoderm. *Development* **130,** 5091–5101 (2003).
17. Cheng, Y., Cheung, M., Abu-Elmagd, M. M., Orme, A. & Scotting, P. J. Chick sox10, a transcription factor expressed in both early neural crest cells and central nervous system. *Brain Res. Dev. Brain Res.* **121,** 233–241 (2000).
18. Dady, A., Blavet, C. & Duband, J. L. Timing and kinetics of E- to N-cadherin switch during neurulation in the avian embryo. *Dev. Dyn.* **241,** 1333–1349 (2012).
19. Esteve, P. & Bovolenta, P. cSix4, a member of the six gene family of transcription factors, is expressed during placode and somite development. *Mech. Dev.* **85,** 161–165 (1999).
20. Groves, a K. & Bronner-Fraser, M. Competence, specification and commitment in otic placode induction. *Development* **127,** 3489–99 (2000).
21. Herbrand, H. *et al.* Two regulatory genes, cNkx5-1 and cPax2, show different responses to local signals during otic placode and vesicle formation in the chick embryo. *Development* **125,** 645–654 (1998).
22. Hu, N., Strobl-Mazzulla, P., Sauka-Spengler, T. & Bronner, M. E. DNA methyltransferase3A as a molecular switch mediating the neural tube-to-neural crest fate transition. *Genes Dev.* **26,** 2380–

5 (2012).
23. Hu, N., Strobl-Mazzulla, P. H., Simoes-Costa, M., Sánchez-Vásquez, E. & Bronner, M. E. DNA methyltransferase 3B regulates duration of neural crest production via repression of Sox10. *Proc. Natl. Acad. Sci. U. S. A.* **111,** 1–6 (2014).
24. Ishihara, T., Ikeda, K., Sato, S., Yajima, H. & Kawakami, K. Differential expression of Eya1 and Eya2 during chick early embryonic development. *Gene Expr. Patterns* **8,** 357–367 (2008).
25. Khatri, S. B. & Groves, A. K. Expression of the Foxi2 and Foxi3 transcription factors during development of chicken sensory placodes and pharyngeal arches. *Gene Expr. Patterns* **13,** 38–42 (2013).
26. Khudyakov, J. & Bronner-Fraser, M. Comprehensive spatiotemporal analysis of early chick neural crest network genes. *Dev. Dyn.* **238,** 716–723 (2009).
27. Litsiou, A., Hanson, S. & Streit, A. A balance of FGF, BMP and WNT signalling positions the future placode territory in the head. *Development* **132,** 4051–62 (2005).
28. Lleras-Forero, L. *et al.* Neuropeptides: developmental signals in placode progenitor formation. *Dev. Cell* **26,** 195–203 (2013).
29. Lunn, J. S., Fishwick, K. J., Halley, P. a & Storey, K. G. A spatial and temporal map of FGF/Erk1/2 activity and response repertoires in the early chick embryo. *Dev. Biol.* **302,** 536–52 (2007).
30. McCabe, K. L., Shiau, C. E. & Bronner-Fraser, M. Identification of candidate secreted factors involved in trigeminal placode induction. *Dev. Dyn.* **236,** 2925–2935 (2007).
31. McKeown, S. J., Lee, V. M., Bronner-Fraser, M., Newgreen, D. F. & Farlie, P. G. Sox10 overexpression induces neural crest-like cells from all dorsoventral levels of the neural tube but inhibits differentiation. *Dev. Dyn.* **233,** 430–44 (2005).
32. McLarren, K. W., Litsiou, A. & Streit, A. DLX5 positions the neural crest and preplacode region at the border of the neural plate. *Dev. Biol.* **259,** 34–47 (2003).
33. Mcmahon, A. R. & Merzdorf, C. S. Early Chick Embryos. 1–12 (2010).
34. Mikawa, T., Poh, A. M., Kelly, K. A., Ishii, Y. & Reese, D. E. Induction and patterning of the primitive streak, an organizing center of gastrulation in the amniote. *Dev. Dyn.* **229,** 422–432 (2004).
35. Niss, K. & Leutz, A. Expression of the homeobox gene GBX2 during chicken development. *Mech. Dev.* **76,** 151–155 (1998).
36. Papanayotou, C. *et al.* A mechanism regulating the onset of Sox2 expression in the embryonic neural plate. *PLoS Biol.* **6,** e2 (2008).
37. Paxton, C. N., Bleyl, S. B., Chapman, S. C. & Schoenwolf, G. C. Identification of differentially expressed genes in early inner ear development. *Gene Expr. Patterns* **10,** 31–43 (2010).
38. Plouhinec, J. L. *et al.* Comparative analysis of gnathostome Otx gene expression patterns in the developing eye: implications for the functional evolution of the multigene family. *Dev. Biol.* **278,** 560–575 (2005).
39. Rex, M. *et al.* Dynamic expression of chicken Sox2 and Sox3 genes in ectoderm induced to form neural tissue. *Dev. Dyn.* **209,** 323–332 (1997).
40. Sato, S. *et al.* Regulation of Six1 expression by evolutionarily conserved enhancers in tetrapods. *Dev. Biol.* **368,** 95–108 (2012).
41. Schlange, T., Andrée, B., Arnold, H. & Brand, T. Expression analysis of the chicken homologue of CITED2 during early stages of embryonic development. *Mech. Dev.* **98,** 157–60 (2000).
42. Schmidt, M., Patterson, M., Farrell, E. & Munsterberg, A. Dynamic expression of Lef/Tcf family members and beta-catenin during chick gastrulation, neurulation, and early limb development. *Dev. Dyn.* **229,** 703–707 (2004).
43. Sheng, G. & Stern, C. D. Gata2 and Gata3: novel markers for early embryonic polarity and for non-neural ectoderm in the chick embryo. *Mech. Dev.* **87,** 213–6 (1999).
44. Streit, A. Extensive Cell Movements Accompany Formation of the Otic Placode. *Dev. Biol.* **249,** 237–254 (2002).
45. Streit, a, Berliner, a J., Papanayotou, C., Sirulnik, a & Stern, C. D. Initiation of neural induction by

FGF signalling before gastrulation. *Nature* **406,** 74–8 (2000).
46. Sweetman, D., Smith, T. G., Farrell, E. R. & Münsterberg, A. Expression of csal1 in pre limb-bud chick embryos. *Int. J. Dev. Biol.* **49,** 427–430 (2005).
47. Tambalo, M. Towards a gene regulatory network for otic and epibranchial specification. *KCL (King's Coll. London)* (2014).
48. Uchikawa, M., Ishida, Y., Takemoto, T., Kamachi, Y. & Kondoh, H. Functional analysis of chicken Sox2 enhancers highlights an array of diverse regulatory elements that are conserved in mammals. *Dev. Cell* **4,** 509–19 (2003).
49. Trevers, K. E. A Cascade of Molecular Events During Neural Induction. *UCl (University Coll. London)* (2015).

Supplementary Table 5. Gene expression table for genes included in the NanoString probe set at primitive streak (HH3-4), PPR (HH5-7) and placode (HH10-12) stages. Blue: expressed; grey: not expressed; white: unknown; aNP: anterior neural plate; aNT: anterior neural tube; aPPR: anterior pre-placodal region; dNT: dorsal neural tube; FB: forebrain; HB: hindbrain; MB: midbrain; MHB: mid hindbrain boundary; p: posterior; pNP: posterior neural plate; pPPR: posterior pre-placodal region; pOP: presumptive olfactory placode; w: weak.

Supplementary Table 6. Analysis of transcription factor binding sites in the Six1-14 enhancer. The 733bp Six1-14 enhancer was analysed using the Cis-eLement OVERrepresentation program using a combined JASPAR and Transfac vertebrate transcription factor binding site library. The sequence was compared to 1000 control shuffles to generate a p-value, the cut-off used was $p<0.05$.

Click here to Download Table S6

.Gene name	EST number	Insert size (bp)
Transcription Factors		
AATF	ChEST771e20	920
ADNP2	ChEST215f16	799
BCL7A	ChEST587h8	535
BCL11A	ChEST779p23	802
BCLAF1	ChEST662a16	730
DBX2	ChEST766g23	776
DLX6	ChEST406p23	793
E2F8	ChEST353j4	697
EAF2	ChEST150c24	638
EZH2	ChEST766d20	676
FLL4	ChEST433o1	815
FOXM1-AUTO1	ChEST977e16	795
FOXN2	ChEST534i24	792
HIF1A	ChEST282l1	630
HMGXB4	ChEST426k11	967
HSF2	ChEST436g19	737
LMX1A	ChEST609m14	726
LZTR1	ChEST589b12	495
MIER1	ChEST98k16	1059
MLLT10	ChEST1013a1	710
MORC2	ChEST972d11	707
MTA3	ChEST312g1	791
MYNN	ChEST536f8	1014
N-MYC	ChEST379n6	675
NFKB1	ChEST491b16	837
NPAS3	ChEST860p24	800
NSD1	ChEST995e21	815
POGZ-AUTO1	ChEST151l19	640
PSIP1	ChEST272n8	914
RRN3	ChEST522o13	852
RYBP	ChEST268o3	841
SOX8	ChEST706o2	778
SOX11	ChEST781p14	680
SOX13	ChEST437d11	788
SP4	ChEST535j5	693
STOX2	ChEST851g13	1500
TBPL1	ChEST72h9	747
TGIF2	ChEST692l13	621
TOX3	ChEST1009p6	983
TRIM24	ChEST401k15	977
VGLL2	ChEST976p9	657

YEATS4	ChEST9i5	756
ZBTB16	ChEST1038b13	594
ZFP161	ChEST309m24	869
ZIC1-AUTO	ChEST459n6	793
ZFHX3	ChEST472l4	733
ZNF217-AUTO1	ChEST192n15	820
ZNF462	ChEST236b12	920
Signalling Molecules		
CXCL14	ChEST896P24	1200
HOMER2	ChEST795g2	846
KREMEN1-LIKE	ChEST751a10	1100
LRP11	ChEST661h3	710
Chromatin modifying enzymes		
CHD7	ChEST757h23	901
DNMT3A	ChEST425j12	890
DNMT3B	ChEST405f22	820
SETD2	ChEST525a17	790
WHSC1	ChEST899n11	860

Supplementary Table 7. List of all EST clones used for in situ hybridisation.